Driving forces in the nano-magnetism world

Intra-atomic exchange, electron correlation effects:

LOCAL (ATOMIC) MAGNETIC MOMENTS

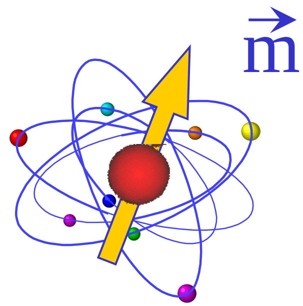

d or *f* electrons

Hund's rules

Inter-atomic exchange:

MAGNETIC ORDER

$$H_{exc} = -\sum_{i \neq j} J_{ij} \mathbf{S}_i \cdot \mathbf{S}_j$$

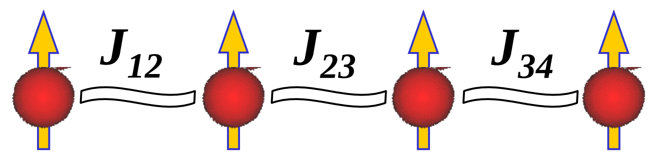

Spin-Orbit Coupling:

MAGNETOCRYSTALLINE ANISOTROPY: K

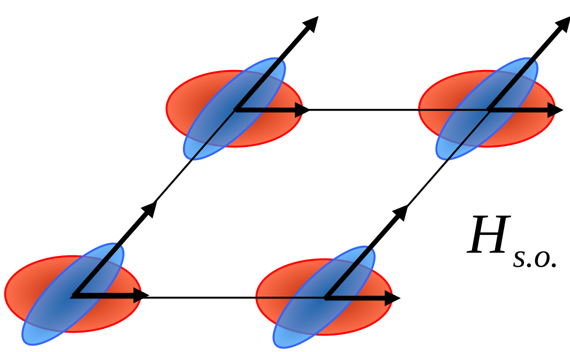

$$H_{s.o.} = \lambda \mathrm{L} \cdot \mathbf{S} = \sum \xi \mathbf{s}_i \cdot \mathrm{l}_i$$

Dipolar Interaction:

SHAPE ANISOTROPY

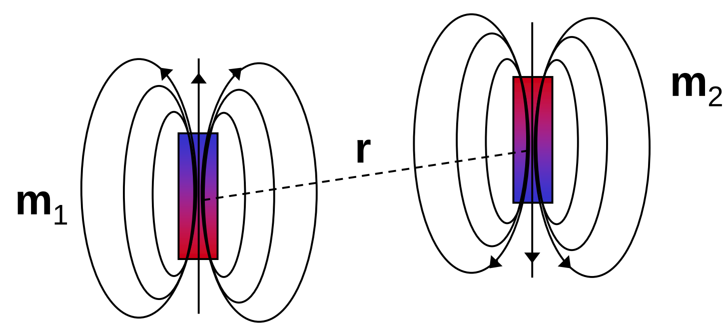

$$H_{dip} = \frac{\mathbf{m}_1 \cdot \mathbf{m}_2}{r^3} - 3\frac{(\mathbf{m}_1 \cdot \mathbf{r})(\mathbf{m}_2 \cdot \mathbf{r})}{r^5}$$

Dipolar interaction

Long range interaction between magnetic moments

$$H_{dip} = \frac{\mathbf{m}_1 \cdot \mathbf{m}_2}{r^3} - 3\frac{(\mathbf{m}_1 \cdot \mathbf{r})(\mathbf{m}_2 \cdot \mathbf{r})}{r^5}$$

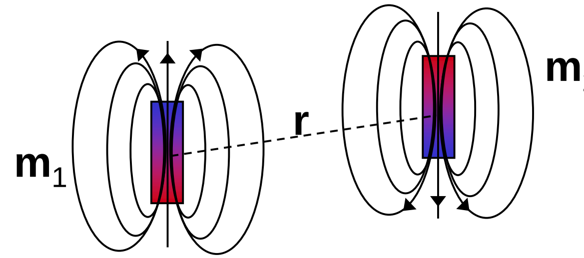

m_1 and m_2 can be the magnetic moments of two atoms in a particle or the moments of two particles

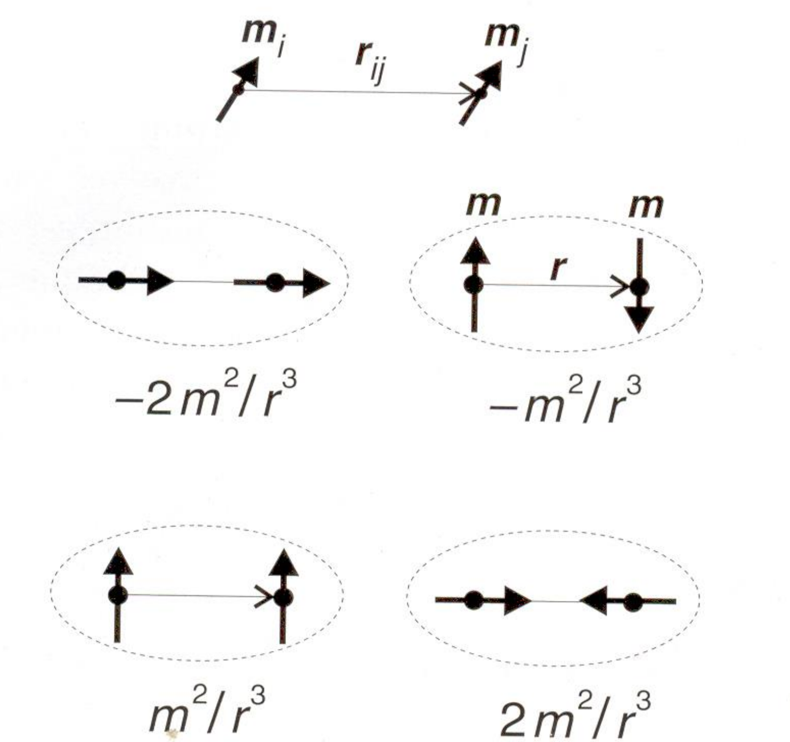

In out-of-plane configuration the dipolar interaction is reduced

The magnetic configurations are determined by the competition, at a local scale, of four different energies:
Zeeman, exchange, magnetocrystalline anisotropy, and dipolar coupling.

$$E = -\mu_0\mu \mathbf{H}\sum_i \mathbf{m}_i - J\sum_{\langle i,j\rangle} \mathbf{m}_i\cdot\mathbf{m}_j - \sum_i k_i(\mathbf{m}_i\cdot\mathbf{e}_i)^2 - \frac{\mu_0\mu^2}{8\pi}\sum_{i,j\neq i}\left[\frac{3(\mathbf{m}_i\cdot\mathbf{r}_{ij})(\mathbf{m}_j\cdot\mathbf{r}_{ij})}{r_{ij}^5} - \frac{\mathbf{m}_i\mathbf{m}_j}{r_{ij}^3}\right],$$

exchange, magnetocrystalline energy -> short range
dipolar energy -> long range

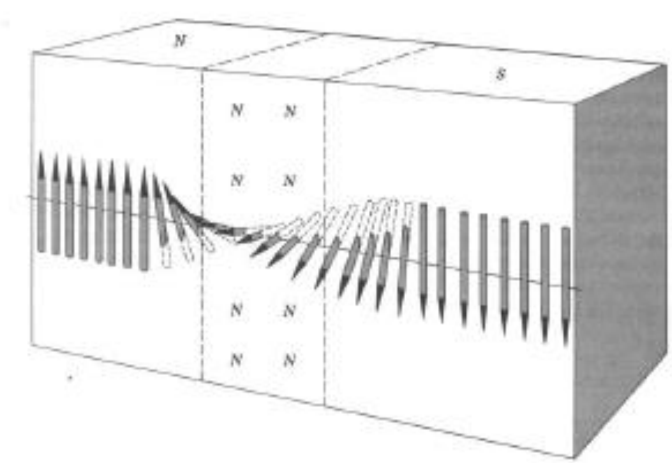

Structure of a domain wall between two ferromagnetic domains with opposite orientation of the local magnetization (180° wall)

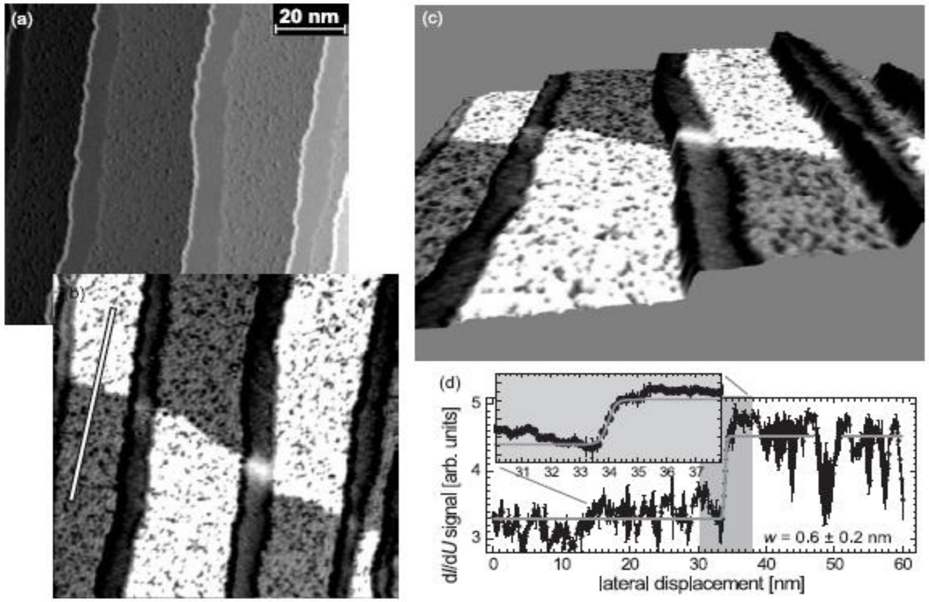

SP-STM of 1.3 monolayers Fe / stepped W(110)

M. Bode, Rep. Progr. Phys. **66**, 523 (2003)

Nanoparticle magnetization state: staid state

Magnetic phase diagram for ultrathin films with perpendicular anisotropy (l_{ex} = 2nm)

R. Skomski et al. Phys.Rev. B **58**, 3223 (1998)
A. Vaterlaus et al. J. Magn. Magn. Mater. **272-276**, 1137 (2004)

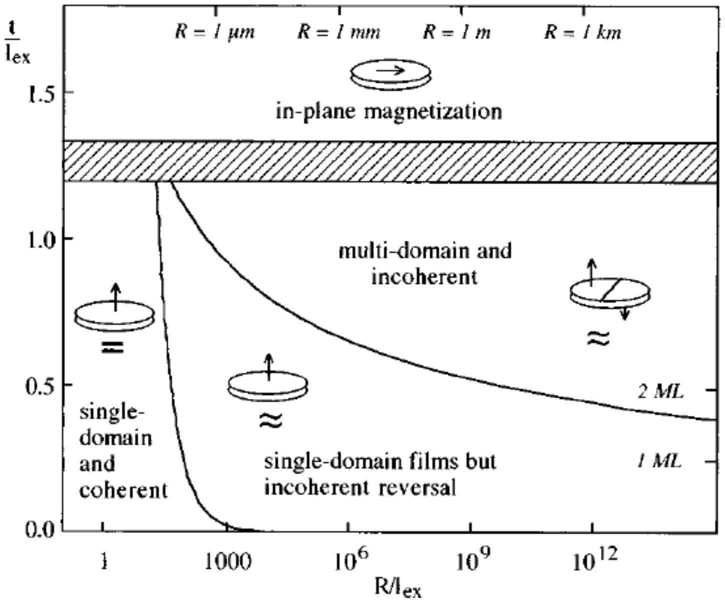

magnetic domain pattern of perpendicularly magnetized ultra-thin Fe particles grown on Cu(0 0 1)

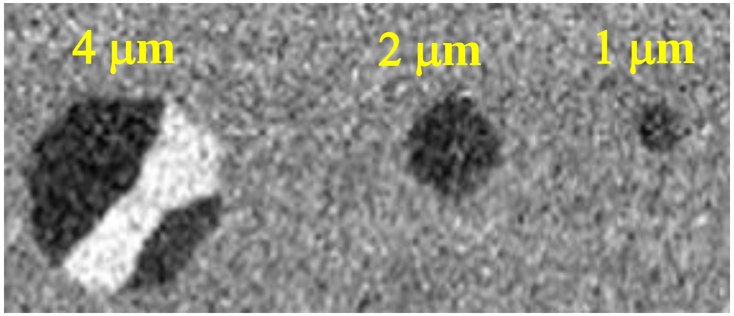

Magnetic phase diagram for ultrathin particles with in-plane anisotropy (Fe/W(001))

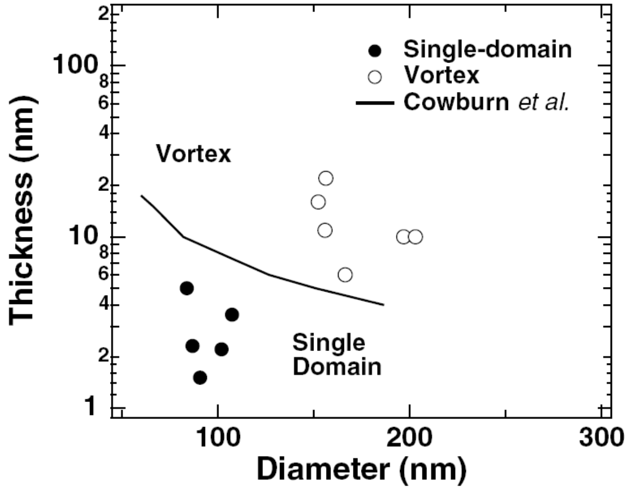

magnetic domain pattern of in-plane magnetized ultra-thin Fe particles grown on W(0 0 1)

SP-STM Calculated vortex

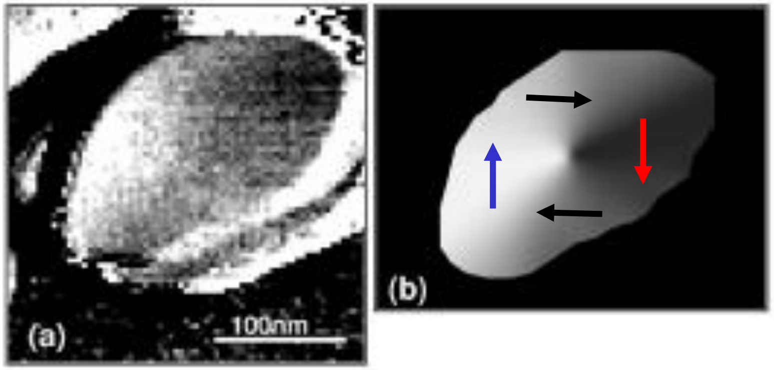

R. Skomski *et al*. Phys.Rev. Lett. **91**, 127201 (2003)

Demagnetizing field: shape anisotropy

$$E_{dip} = -\frac{\mu_0}{2}\int \mathbf{M}\cdot\mathbf{H}_{dem}\,dV$$

$$\mathbf{H}_{dem} = -\mathbf{D}\,\mathbf{M}$$

Pushes the magnetization M along the longer side of the nanostructure:
Cylinder -> M // axis
Disk -> M // disk surface

Sphere:

$$D = \begin{bmatrix} \frac{1}{3} & 0 & 0 \\ 0 & \frac{1}{3} & 0 \\ 0 & 0 & \frac{1}{3} \end{bmatrix}$$

∞-Cylinder:

$$D = \begin{bmatrix} \frac{1}{2} & 0 & 0 \\ 0 & \frac{1}{2} & 0 \\ 0 & 0 & 0 \end{bmatrix}$$

∞-Plane (thin film):

$$D = \begin{bmatrix} 0 & 0 & 0 \\ 0 & 0 & 0 \\ 0 & 0 & 1 \end{bmatrix}$$

Co/Pt(111)

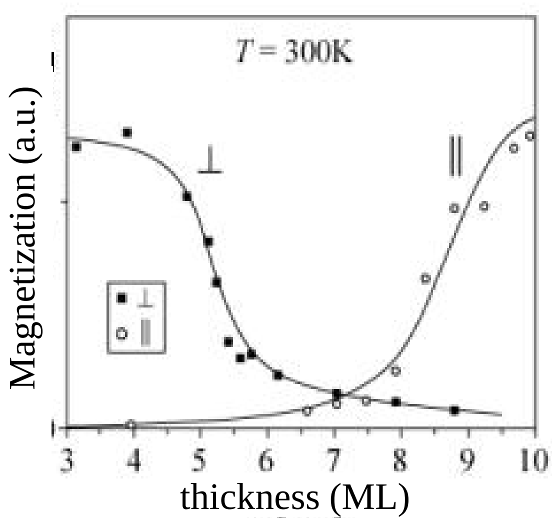

Orientation and shape of Co magnetic domains

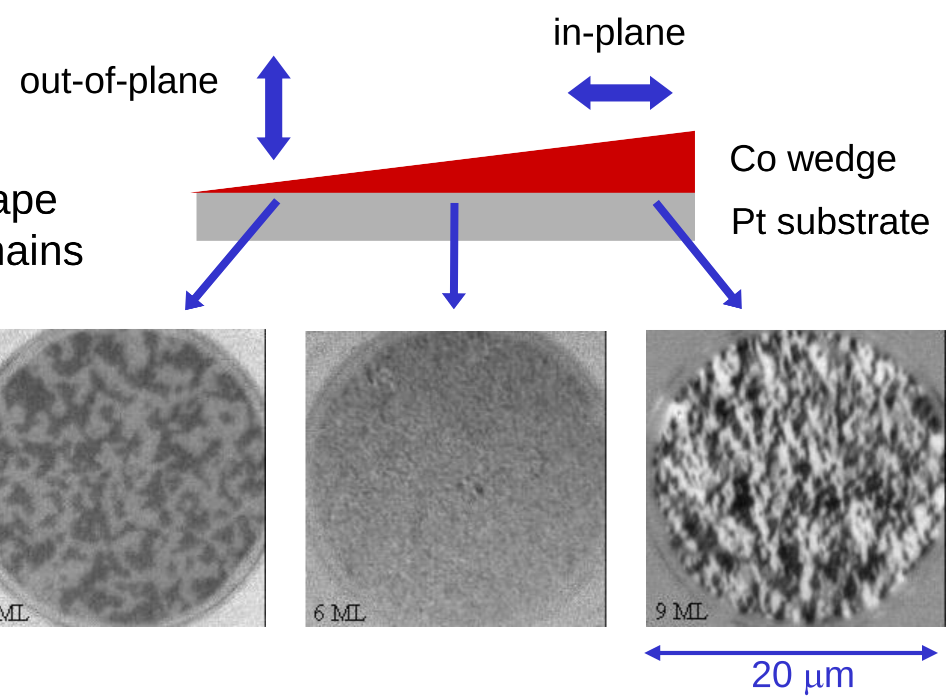

X-ray photoemission electron microscopy, SIM beamline @ Swiss Light Source

Thermal stability of a cluster magnetization vs MAE

A bit is a binary system where 1 and 0 correspond to the magnetization being up or down → Magnetization along a defined axis: easy magnetization axis

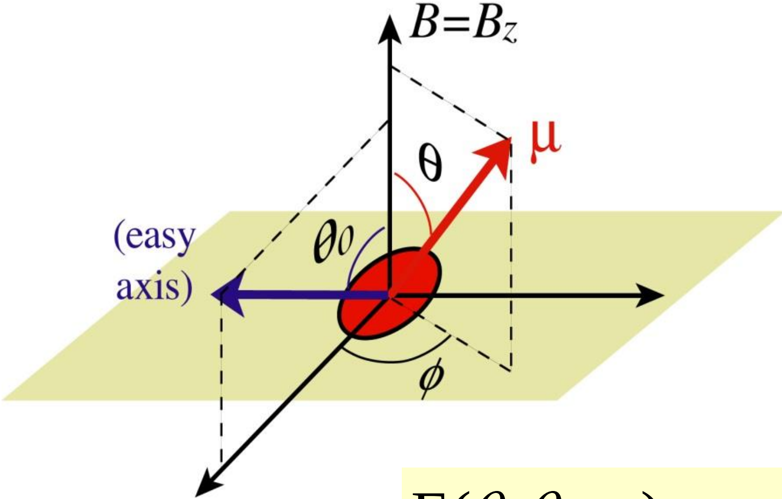

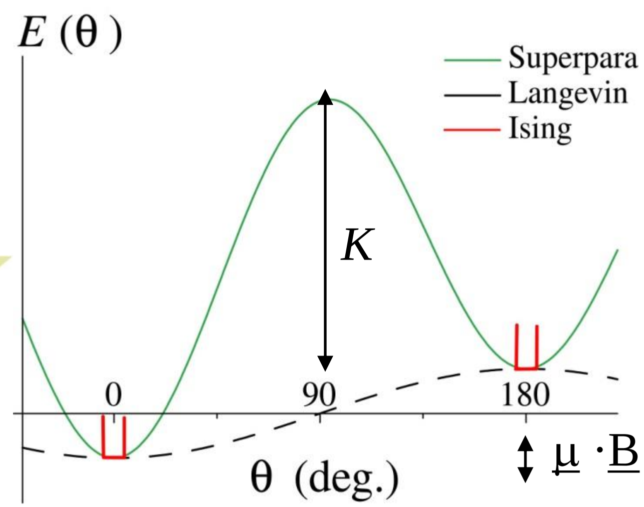

$$E(\theta,\theta_0,\varphi) = -\boldsymbol{\mu}\cdot\mathbf{B} - K\cos^2(\mathbf{easy}\cdot\boldsymbol{\mu})$$

Reversal energy barrier

assuming a coherent magnetization reversal (i.e. all spins turning at the same time) K is the MAE

Magnetic anisotropy energy and superparamagnetic limit

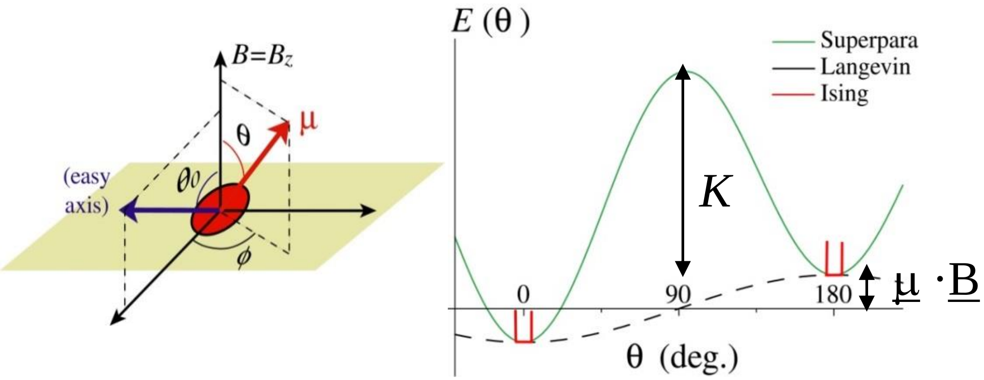

$$E(\theta,\theta_0,\varphi) = -\boldsymbol{\mu}\cdot\mathbf{B} - K\cos^2(\mathbf{easy}\cdot\boldsymbol{\mu})$$

Avg. time (relaxation time) taking to jump from one minimum to the other:

$$\tau = \tau_0 \exp(K/kT) \quad \tau_0 \approx 10^{-10}\text{s}$$

τ = 1 year → K = 40 kT

τ = 1 second → K = 23 kT

The magnetic anisotropy energy determines the lifetime of the magnetic state

Blocking temperature T_b

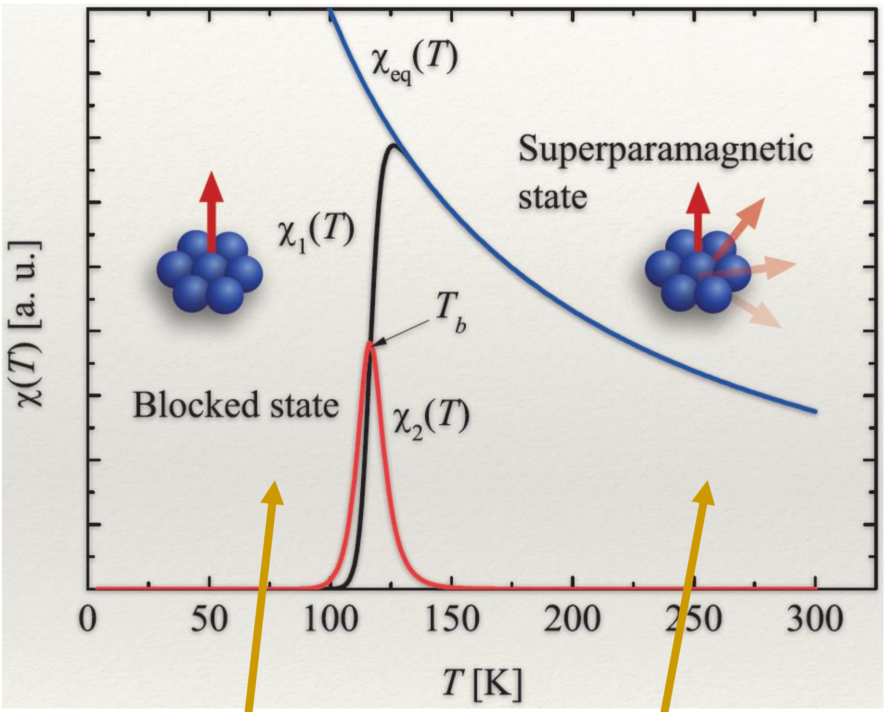

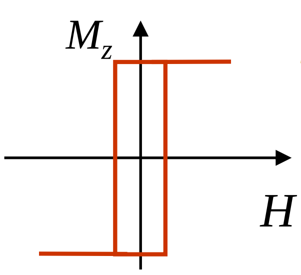

Blocking: K/kT >>30

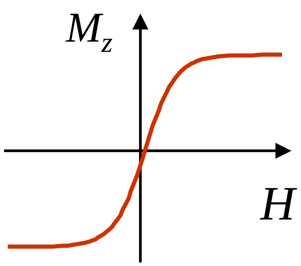

Superparamagnetic: K/kT <<30

Coherent reversal: T = 0

Single-domain particles: the Stoner-Wohlfart model

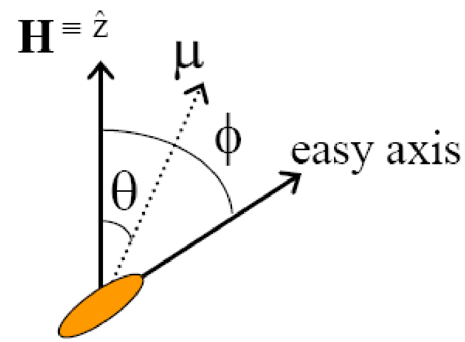

Magnetization of a single-domain particle in an external field.

$$E = E_{Zeeman} + E_{mc} + E_{dm}$$

Suppose $\mu = MV$ = const. for any H value (coherent rotation) and, for simplicity, $E_{dm} = 0$. $E_{mc} = K_1 V$

$$E = -\mu H \cos\theta - K_1 V \cos^2(\theta - \phi) \qquad (1)$$

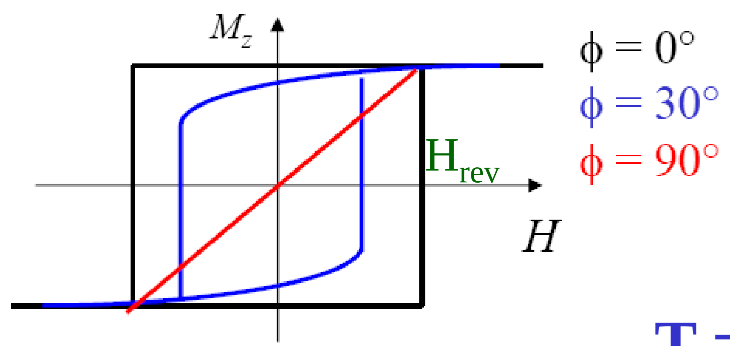

The magnetiic moment $\mu = MV$ will point along a direction that makes E a minimum:

$$\frac{\partial E}{\partial \vartheta} = \mu H \sin\vartheta + K_1 V \sin(2(\vartheta - \varphi)) = 0 \qquad (2)$$

T = 0

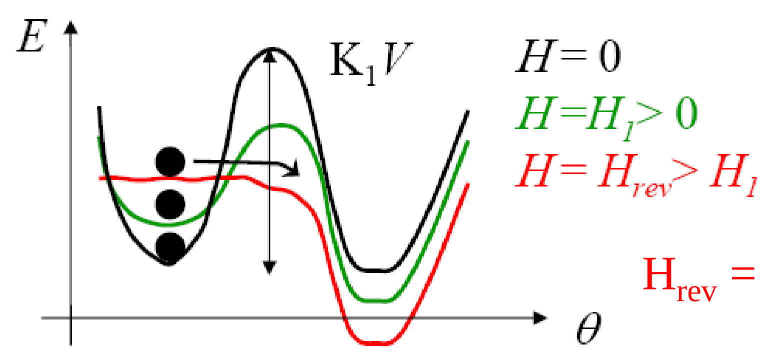

Eq. 2 can be solved for θ and we can plot $M_z = M\cos\theta$ (this is what one usually measures) as a function of H.

The reversal field is the field at which the energy minimum in eq. (1) vanishes ($\partial^2 E/\partial\vartheta^2 = 0$)

$$H_{rev} = 2K_1/M$$

During the magnetization reversal all the atom spins in the particle stay aligned

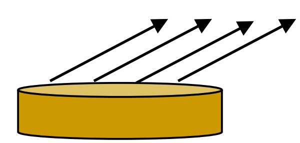

Coherent reversal: T ≠ 0

Field orientations and sweep rate effects on magnetic switching of Stoner–Wohlfarth particles[a)]

Jing Ju Lu, Huei Li Huang, and I. Klik
Department of Physics, National Taiwan University, Taipei, Taiwan 10764, Republic of China

The hysteresis loop for an ensemble of noninteracting monodomain particles (containing *s* atoms each of them having magnetic moment *m*) and with uniaxial anisotropy represents the asymmetry in the number of particles pointing up $n\uparrow$ and down $n\downarrow$ changing over time with the applied field

$$\frac{dn_\uparrow}{dt} = -\kappa_{\uparrow\downarrow} n_\uparrow + \kappa_{\downarrow\uparrow} n_\downarrow$$

$$\kappa_{\uparrow\downarrow} = \nu_0 e^{-E_{\uparrow\downarrow}/k_B T}$$

$$E_{\uparrow\downarrow} = K\sin^2\vartheta - s\,m\,H\cos(\vartheta-\varphi)$$

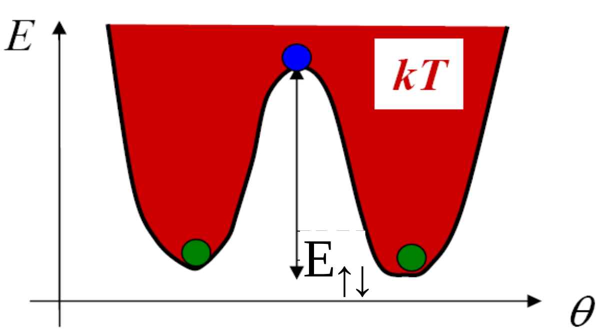

J. J. Lu *et al.*, J. Appl. Phys. **76**, 1726 (1994)

1.1 ML Co/Au(11,12,12)
Two atomic layer high particles
s = 600 atoms

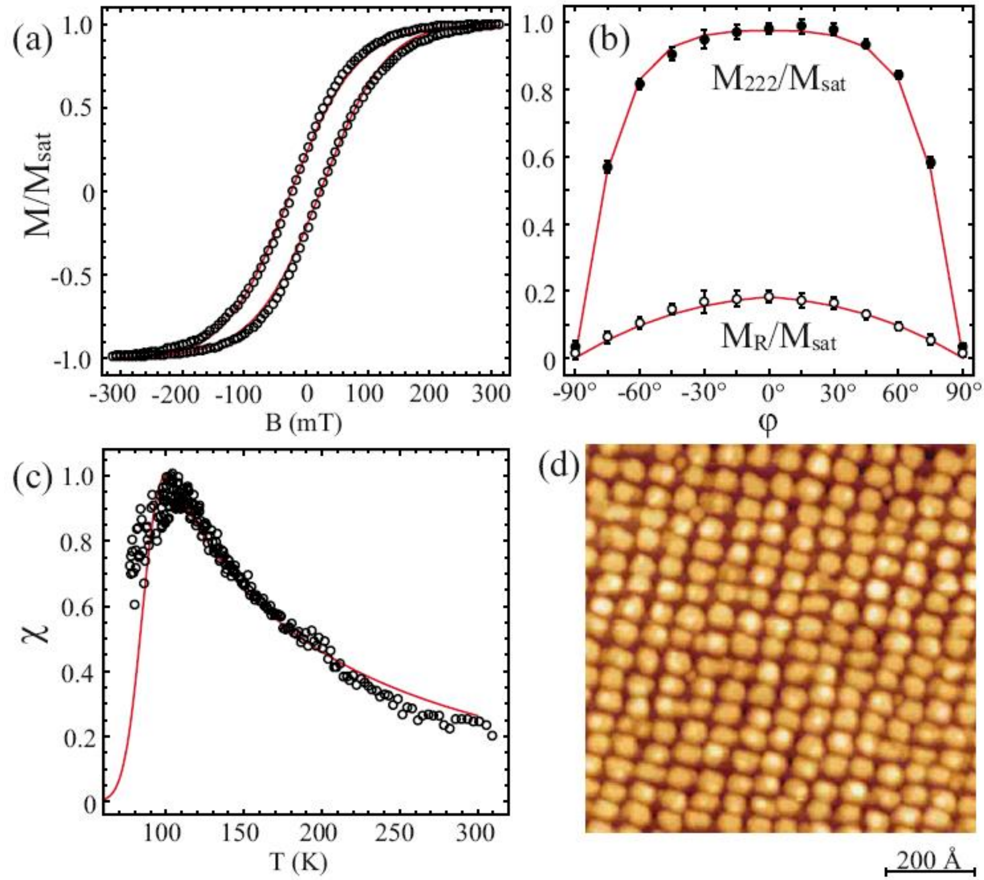

A. Lehnert *et al.*, Rev. Sci. Inst. **80**, 023902 (2009)

Nanomagnets: fundamental limits

What is the smallest size of a ferromagnetic particle at room temperature?

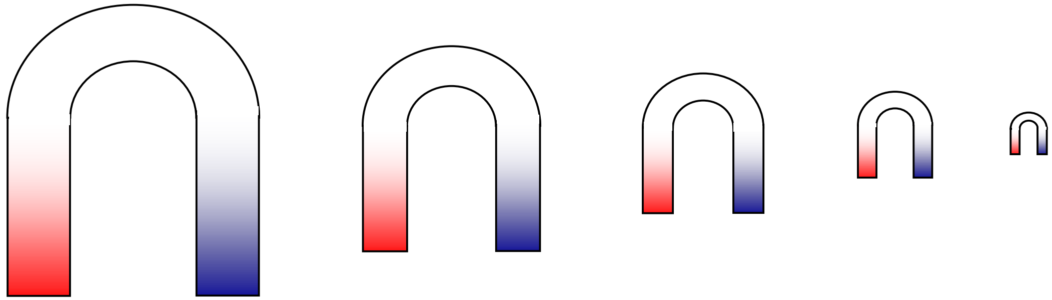

$nK > 1$ eV

- K → magnetic anisotropy energy per atom
- n → number of atoms

K = magneto-crystalline anisotropy + shape anisotropy (usually small)

Co atoms on Pt(111) with 2-fold coordination: K = 3 meV/atom, ***n* = 350 atoms**

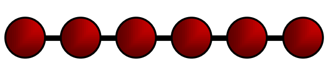

1D chain

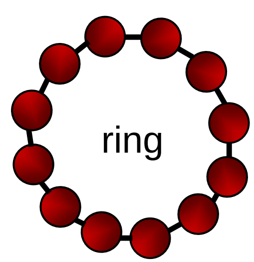

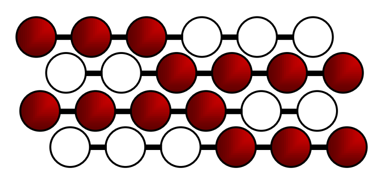

"labyrinth" lattice

Nano-enginering:Pt core and Co shell

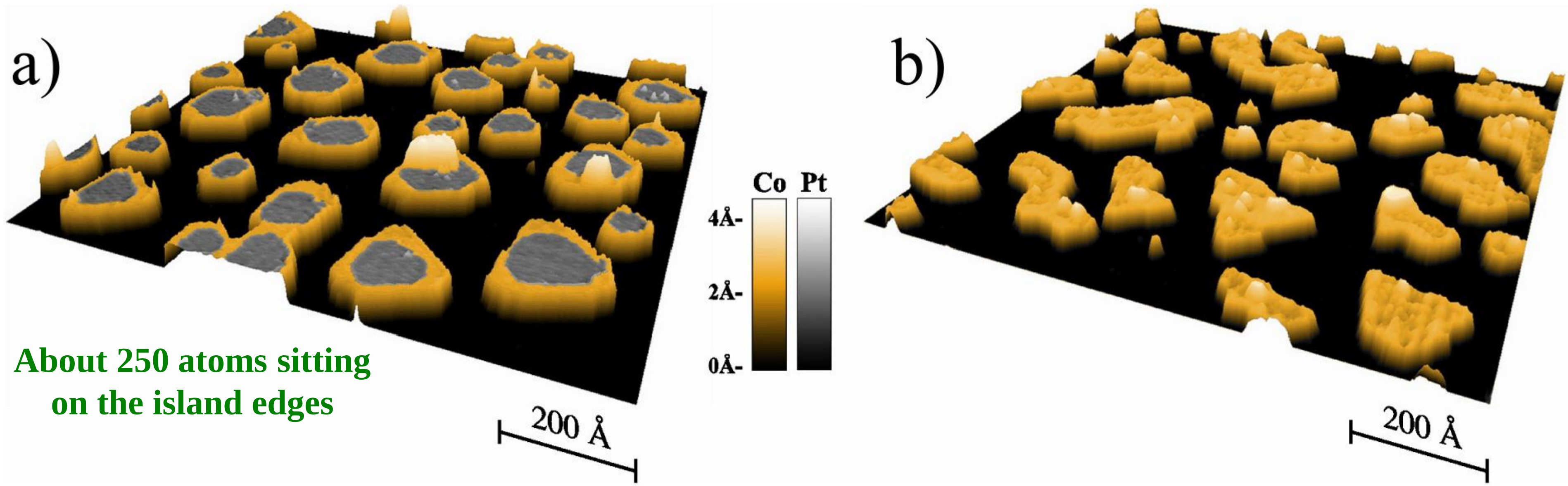

About 250 atoms sitting
on the island edges

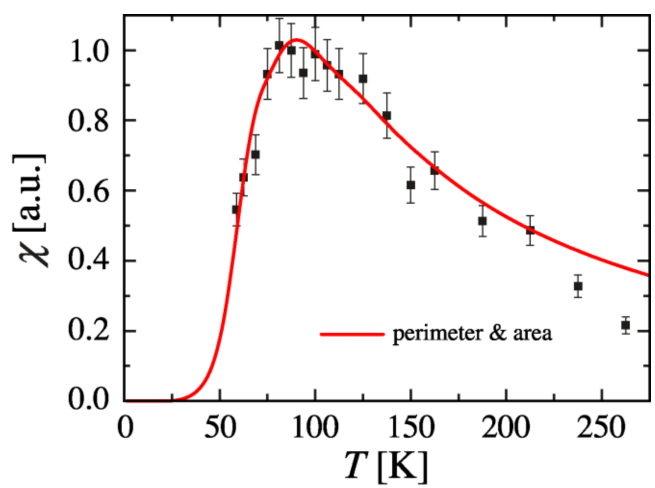

MOKE susceptibility

(same blocking temperature T_b)

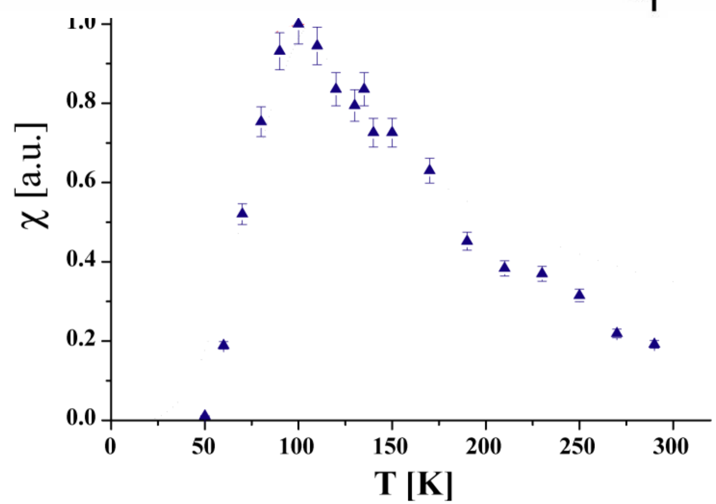

Compared to pure Co islands:

1) same total MAE (0.9 meV/edge-atom)

2) reduced magnetic moment

S. Rusponi et al., *Nature Mat*. **2**, 546 (2003).

Nano-enginering: interline effect

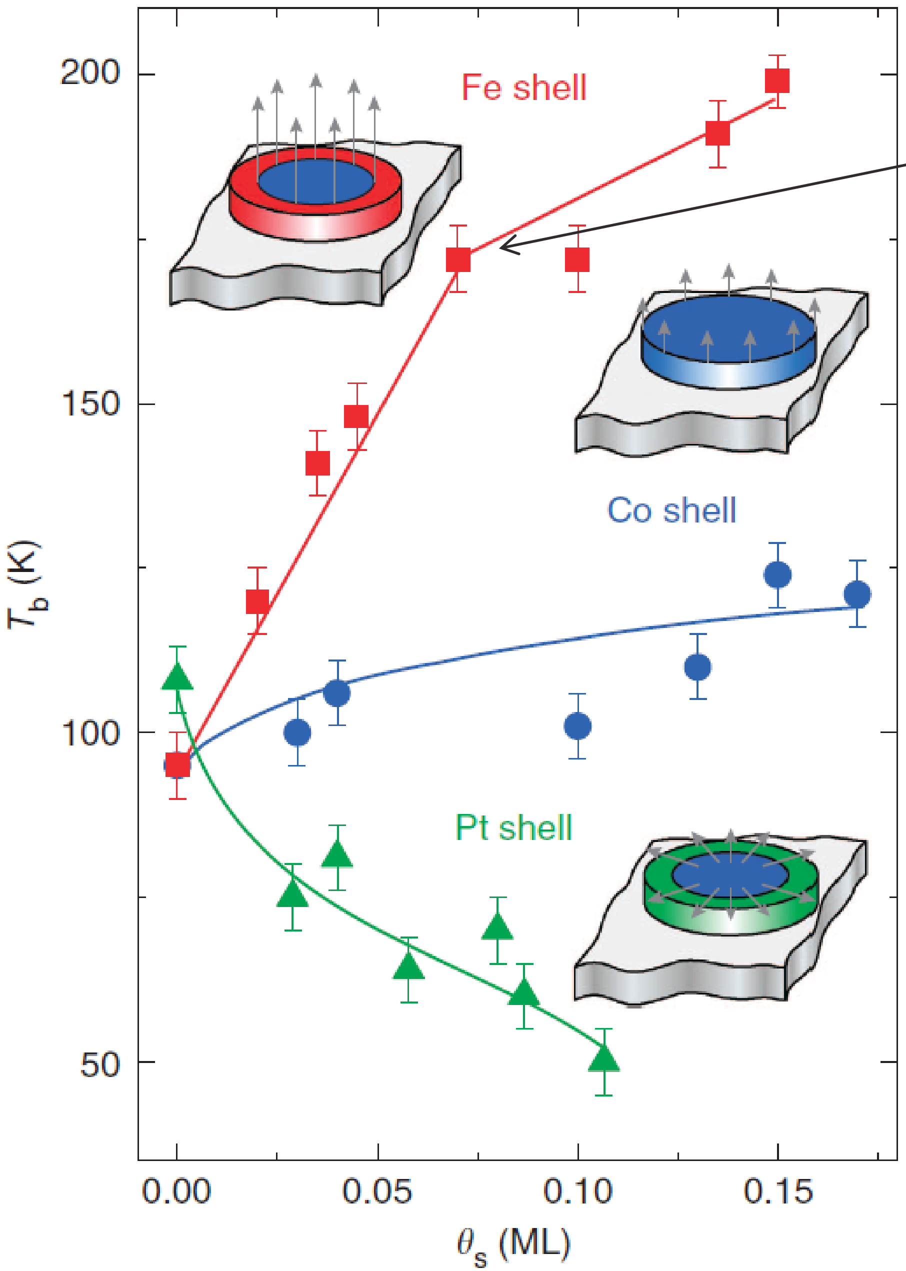

In the mean the rim has a width of two atoms

But….

Real island shape at θ_s = 0.04 ML

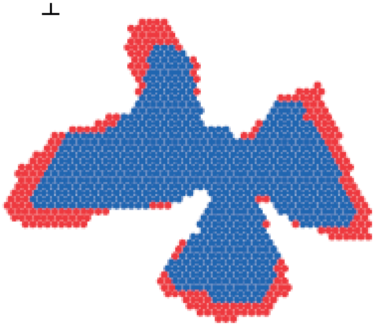

S. Ouazi et al., *Nature Commun*. **3**, 1313 (2012).

Nano-enginering: inteface effect

Interline decreases T_b (similar to Pt case)

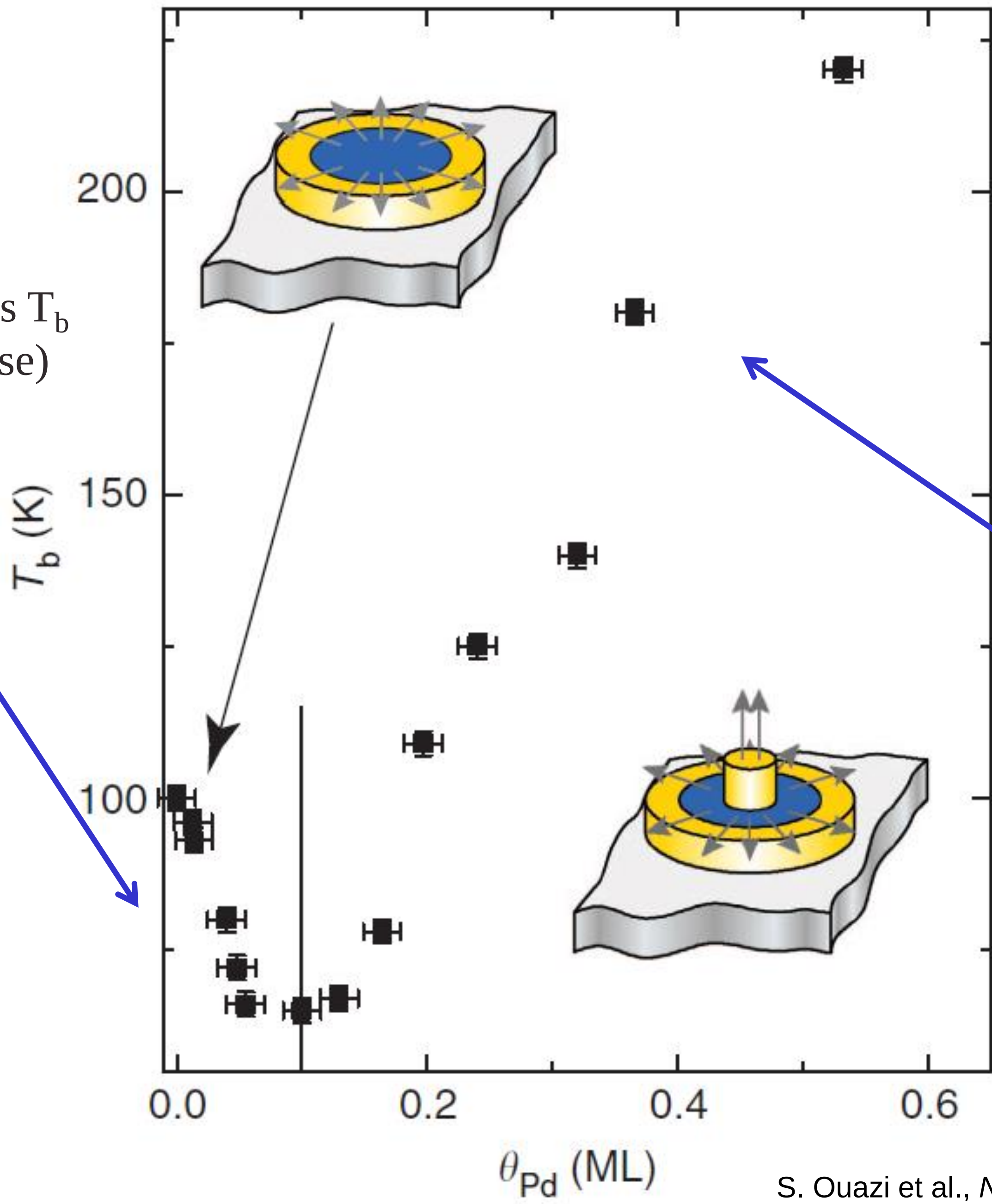

Interface increases T_b

S. Ouazi et al., *Nature Commun*. **3**, 1313 (2012).

Nano-enginering: combining interline and interface effects

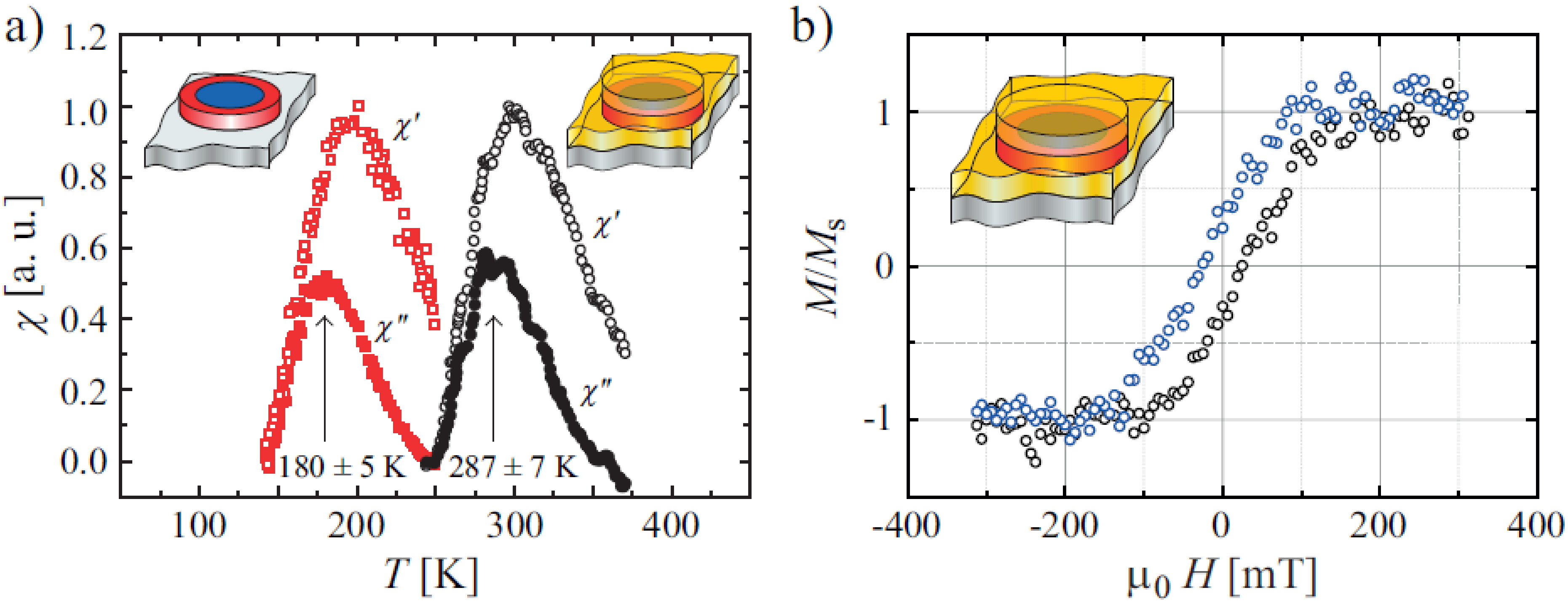

Islands containing about 1300 atoms with T_b close to room T

S. Ouazi et al., *Nature Commun*. **3**, 1313 (2012).

Lattice of magnetic dots: dipolar interaction

Au(788) vicinal surfaces

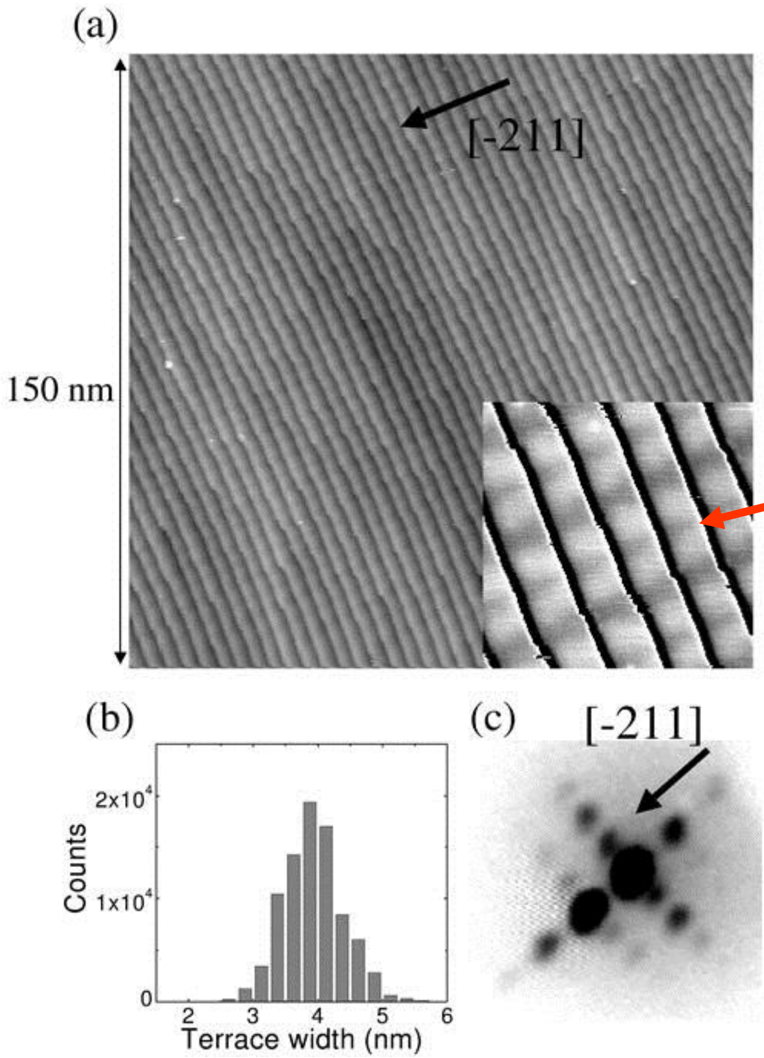

(111)-oriented terraces with reconstruction lines perpendicular to step edges

Surface reconstructions on two consecutive terraces are coherent

Co nucleates in bi-layer dots where the reconstruction lines cross the step edges

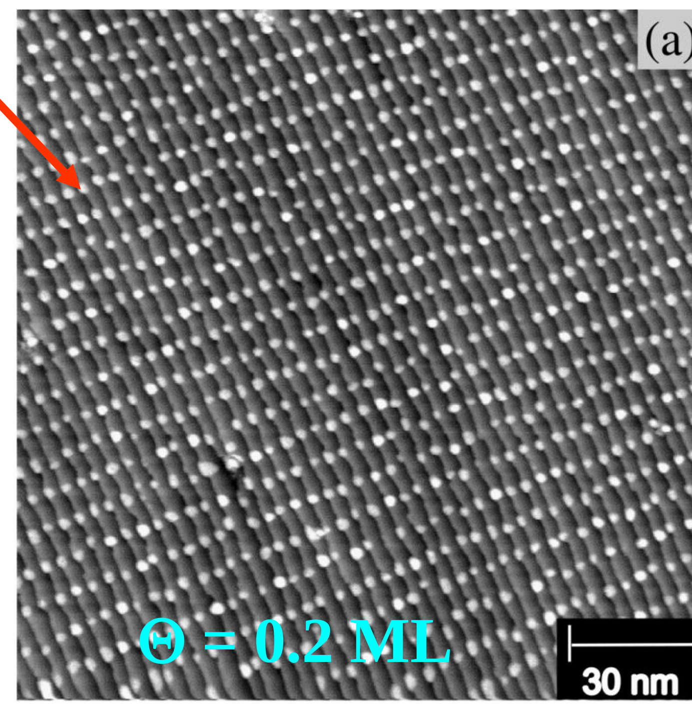

V. Repain et al. Europhys. Lett. **58**, 730 (2002)

Ultra-high density Co clusters superlattices on Au(788)

MAE distribution narrower than size distribution

0.75 ML Co

For circular particle ΔN/N = 2 Δp/p

Uniaxial
out-of-plane
easy axis => one
particle per bit

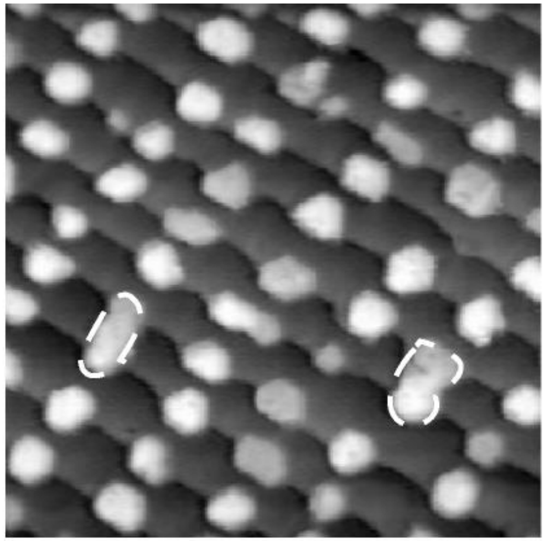

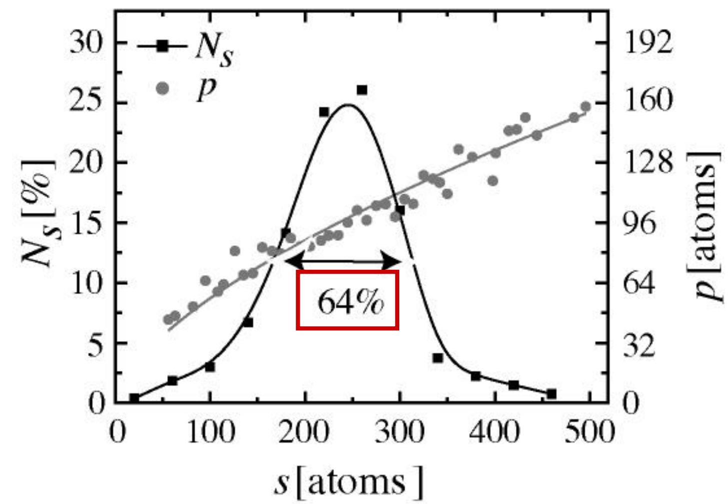

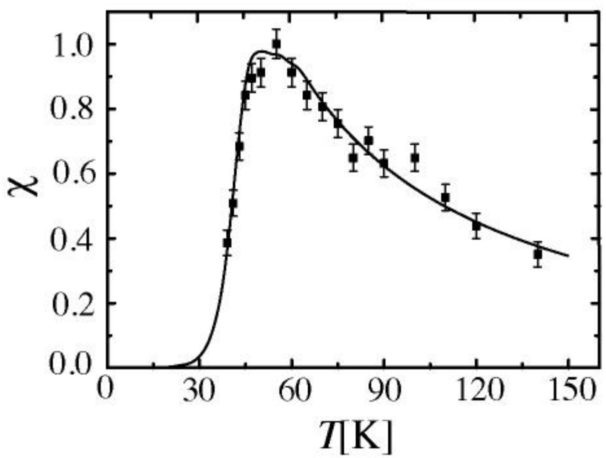

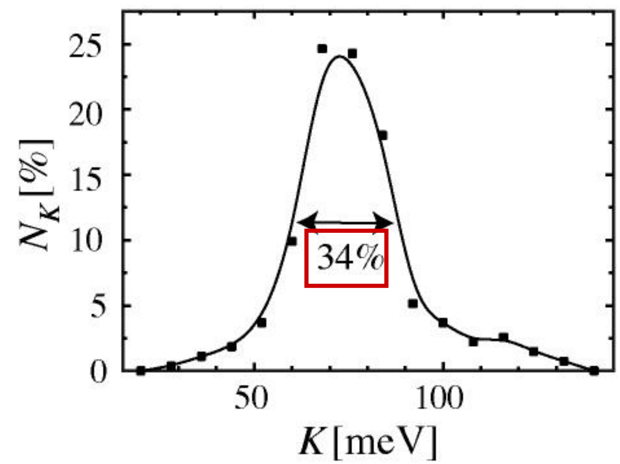

N. Weiss et al. Phys.Rev. Lett. **95**, 157204 (2005)

Unprecedented narrow MAE distribution

Ultra-high density Co clusters superlattices on Au(788)

Negligible dipolar interaction at
26 Tdots/in^2

Switching field H_{sw} = 2K/M = 4 T
Dipolar field < 0.04 T

0.75 ML Co

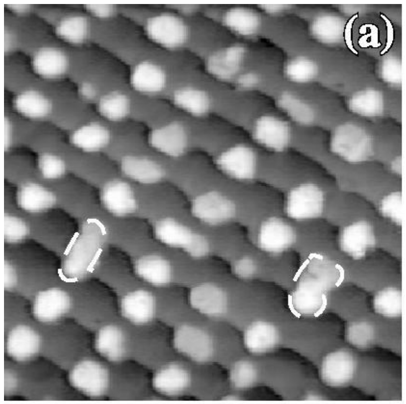

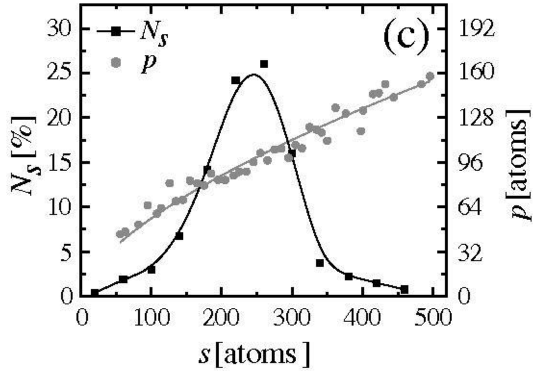

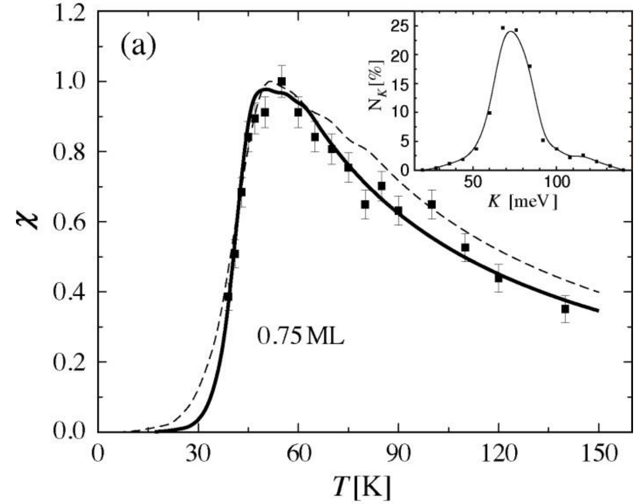

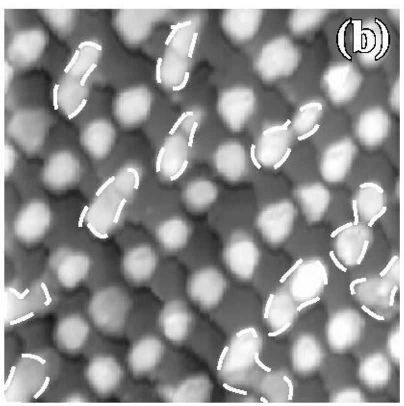

1.1 ML Co

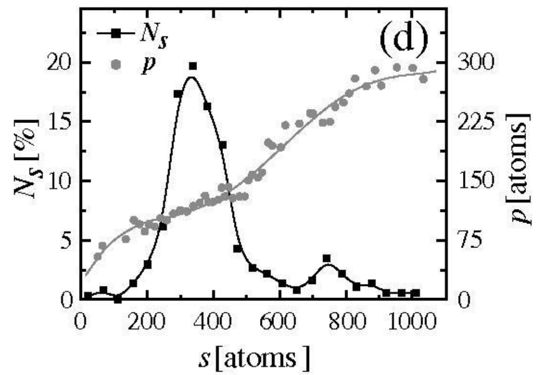

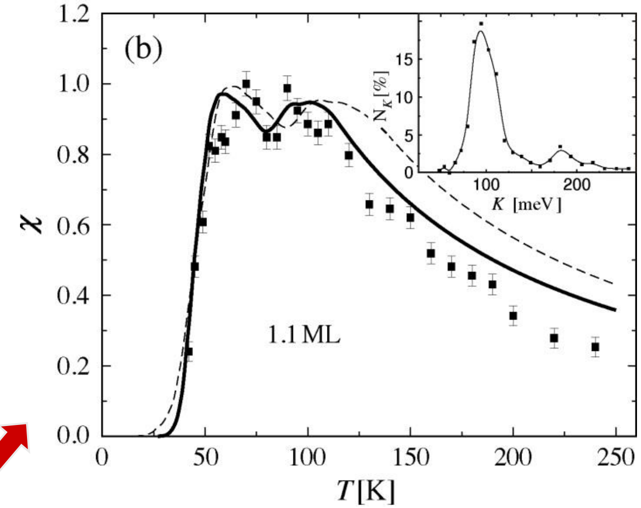

Bimodal size distribution

Bimodal χ vs. T

Self-assembly of colloid particles

Particles with organic capping

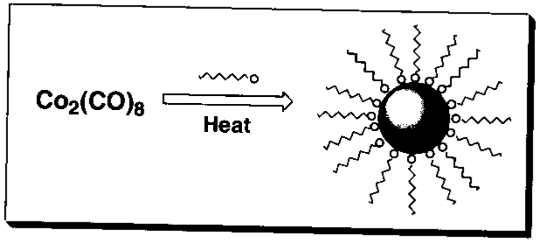

Self-assembly *via* solvent evaporation

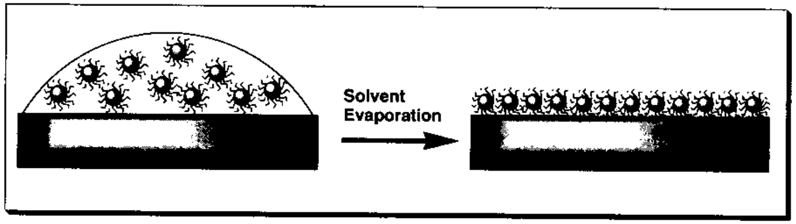

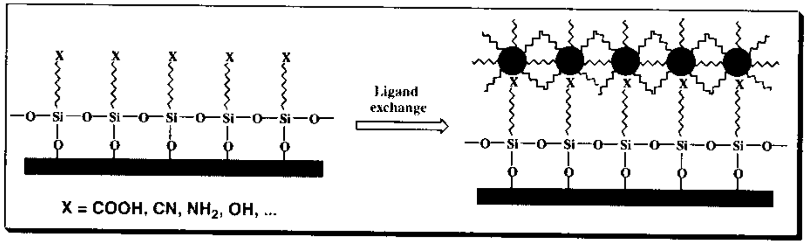

Assembly onto functionalized substrate
via ligand exchange

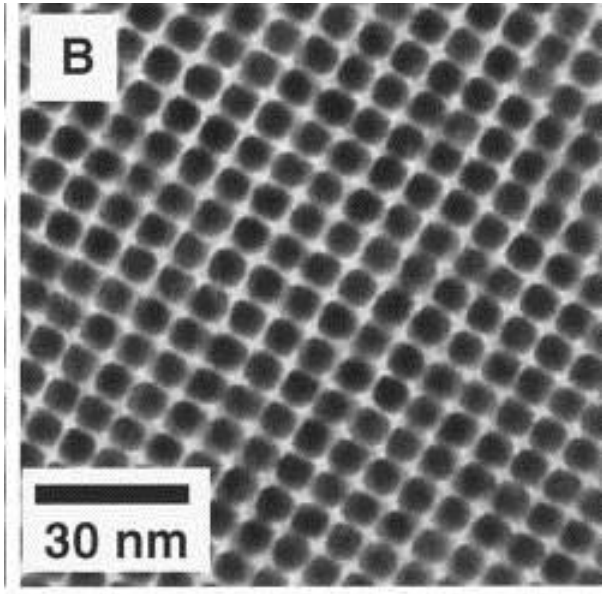

Tunable size in the range 1-10 nm

Control of the particle volume:
HWHM = 15-20 %

Organic capping used as a spacer
to define the array density

Magnetism of colloid particles

4 nm $Fe_{56}Pt_{44}$ annealed particles ($L1_0$ phase)

MAE ≈ 48 kT

Stability criterion at room temperature: MAE = 40 kT

S. Sun *et al.*, Science **287**, 1989 (2000)

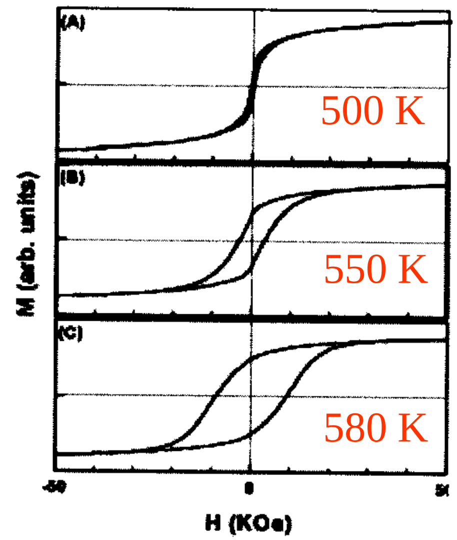

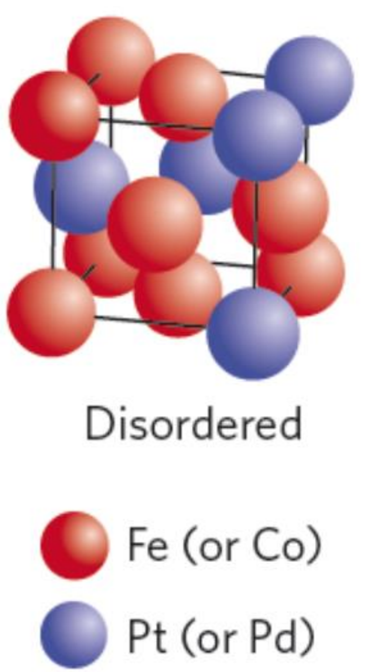

Annealing to about 600°C

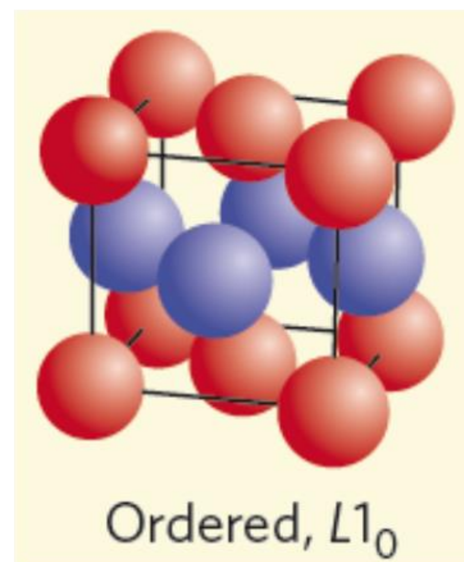

Magnetism of colloid particles: drawbacks

1) Randomly oriented easy axis

SNR requires more than one particle per bit

Density limit: 1 Tbit/in^2

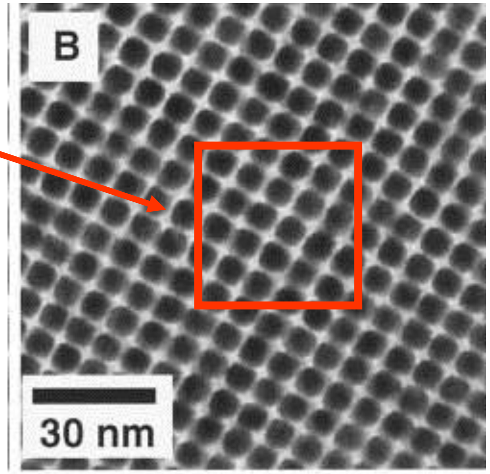

2) Relatively large MAE distribution

10 year stable

1 hour stable

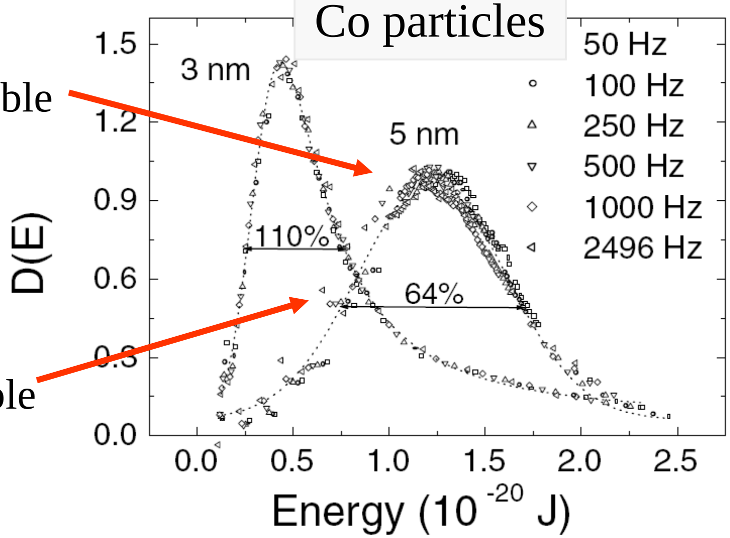

S. I. Woods *et al.*, PRL **87**, 137205 (2001)

3) Order lost after annealing

T= 20°C

T= 530°C

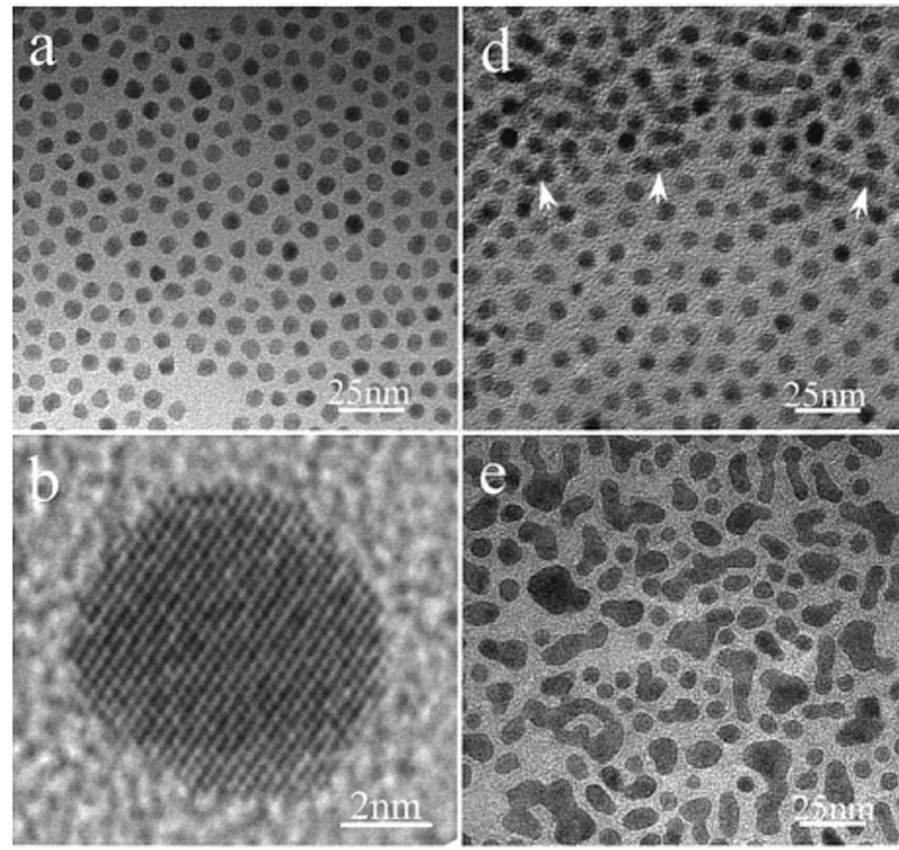

T= 600°C

N. Blanc, PhD thesis (Lyon dec 2009)

Beating the superparamagnetic limit with exchange bias

Co particles in a CoO matrice

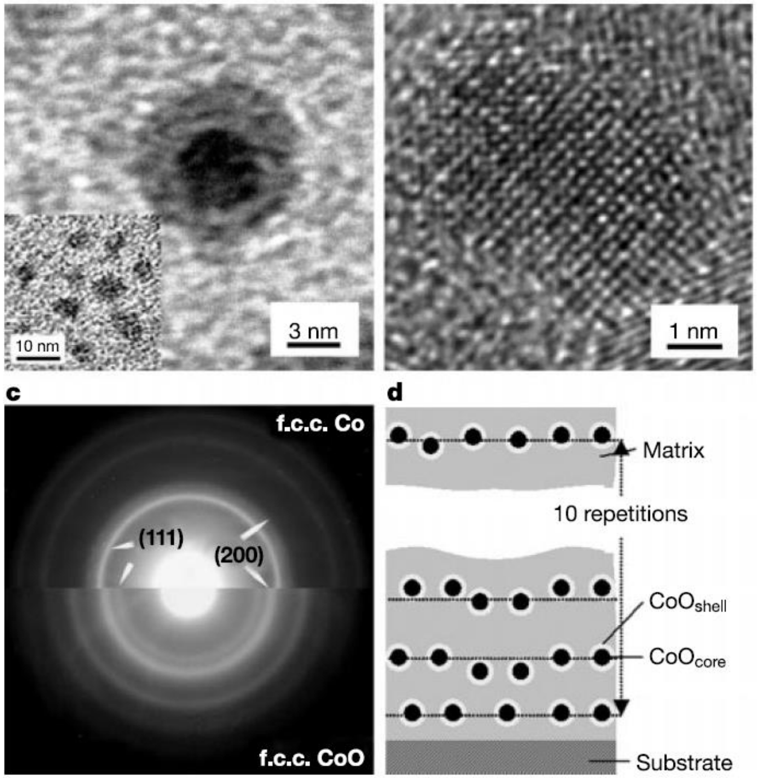

Co in Al2O3 matrice

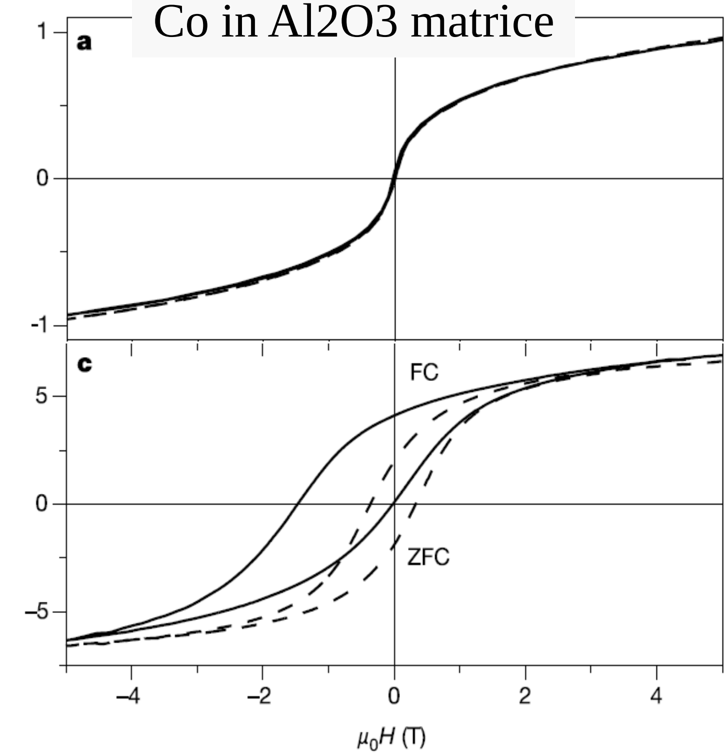

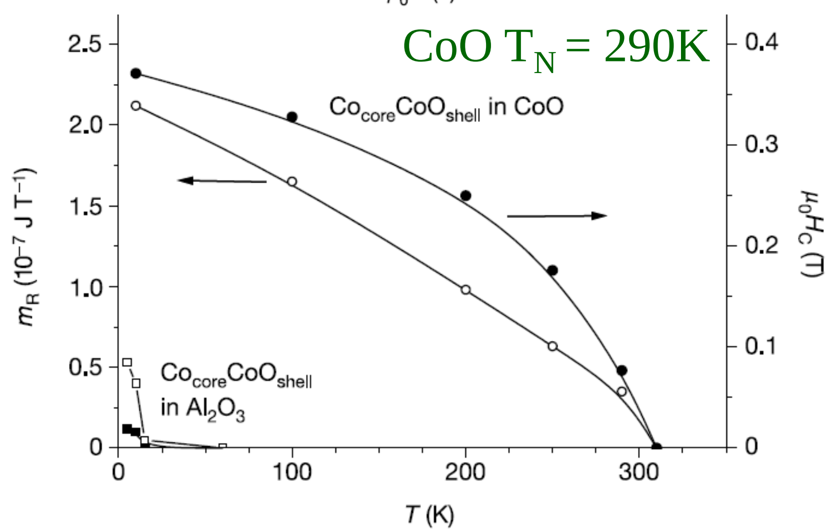

Scheme of a writing procedure: the bias field depends on the versus of the external field during cooling

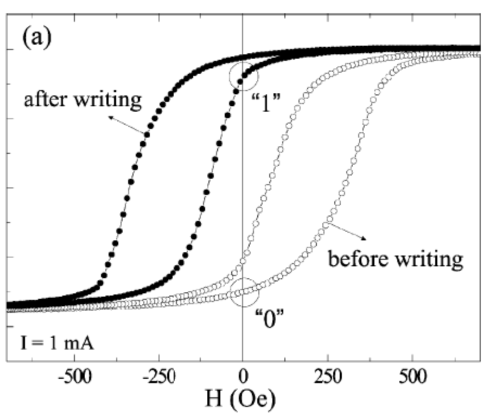

V. Skumryev *et al.*, Nature **423**, 850 (2003)

Site selective nucleation at dislocation elbows on Au(111)

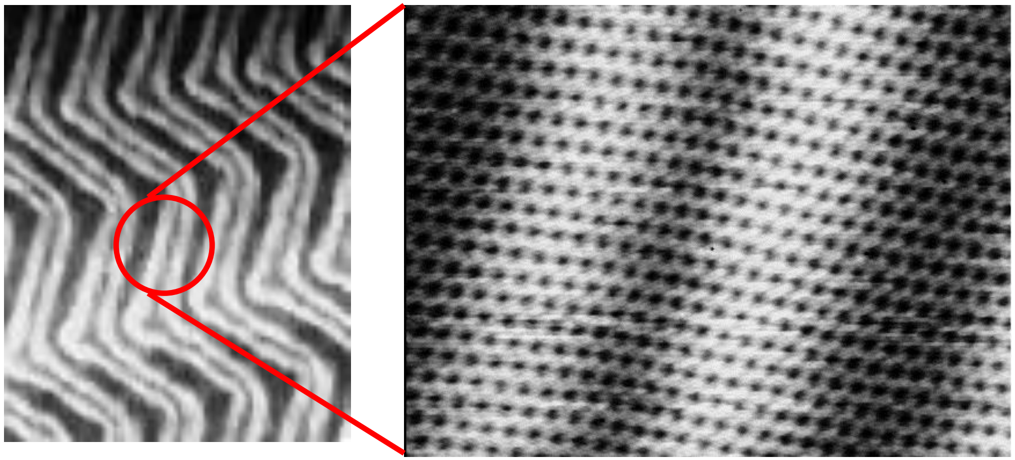

J.V. Barth *et al.*, PRB **42**, 9307 (1990)

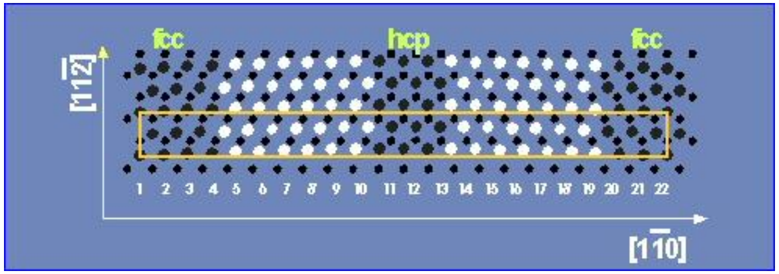

The Au(111) herringbone reconstruction: 23 surface atoms on top of 22 second layer atoms result in partial dislocations that separate fcc and hcp regions.

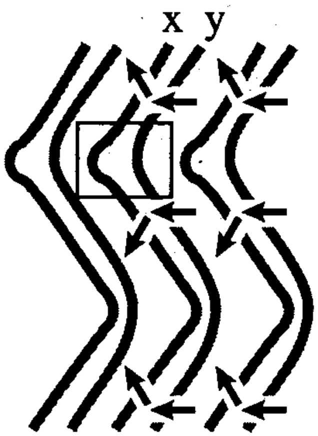

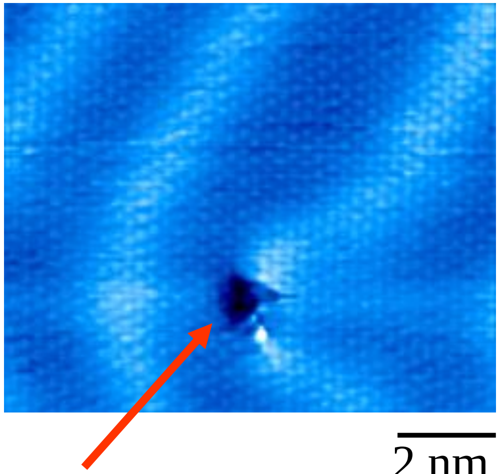

2 nm

Nucleation triggered by exchange

[courtesy S. Rousset, CNRS, Univ. Paris 7 and 6]

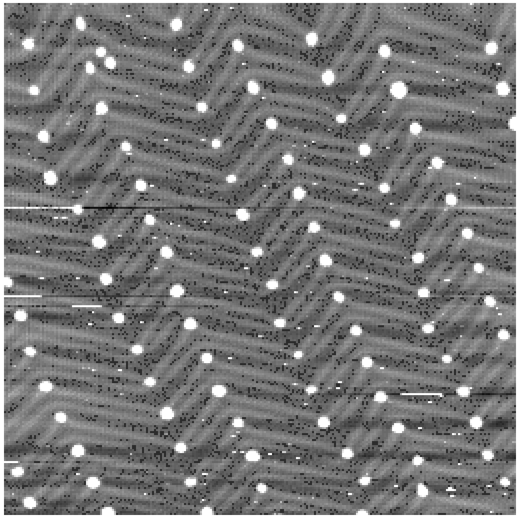

20 nm

Co clusters on Au(111) T = 300 K

NANO INSTITUT DE PHYSIQUE DES NANOSTRUCTURES

Co pillars on Au(111)

EPFL École Polytechnique Fédérale de Lausanne

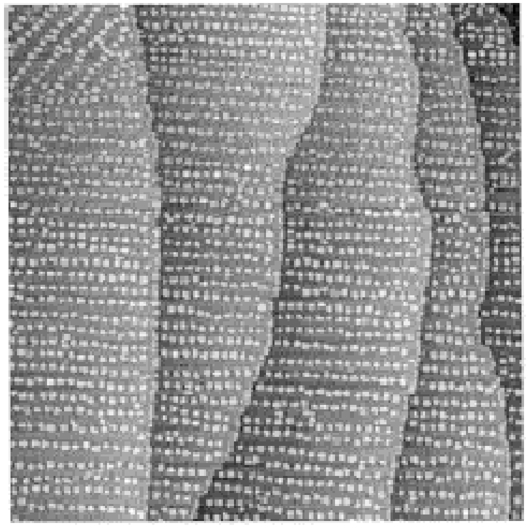

(a) 300×300 STM image after deposition of 0.2 ML of Co at 300 K on Au(111)

(b) after deposition of Au up to the fourth ML, performed while raising the temperature from 425 to 475 K

(c) after another deposition of 0.2 ML of Co at 500 K.

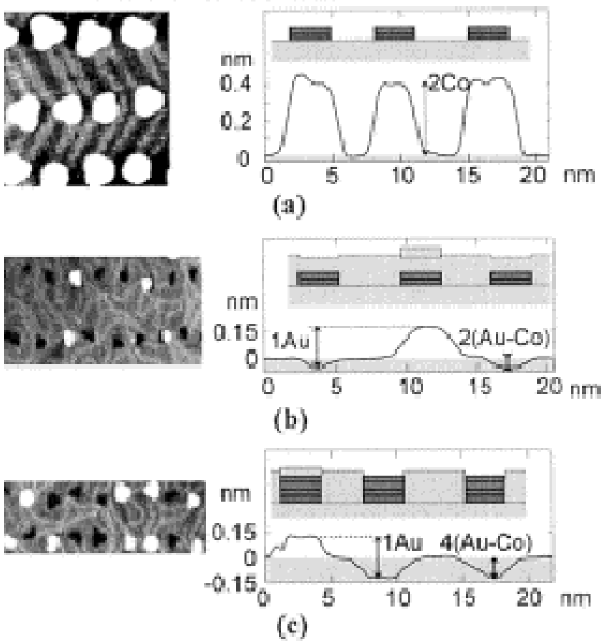

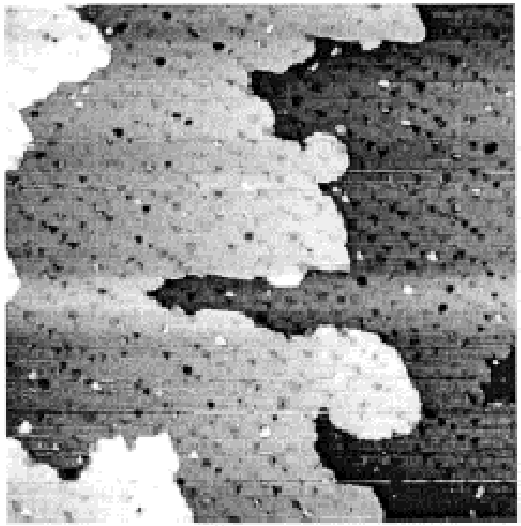

Final result: 300×300 STM image after 0.2 ML of Co have been piled one on top of the other.

O. Fruchart *et al*., PRL **83**, 2769 (1999)

Co pillars on Au(111)

Pillar height adjusted to select the blocking temperature

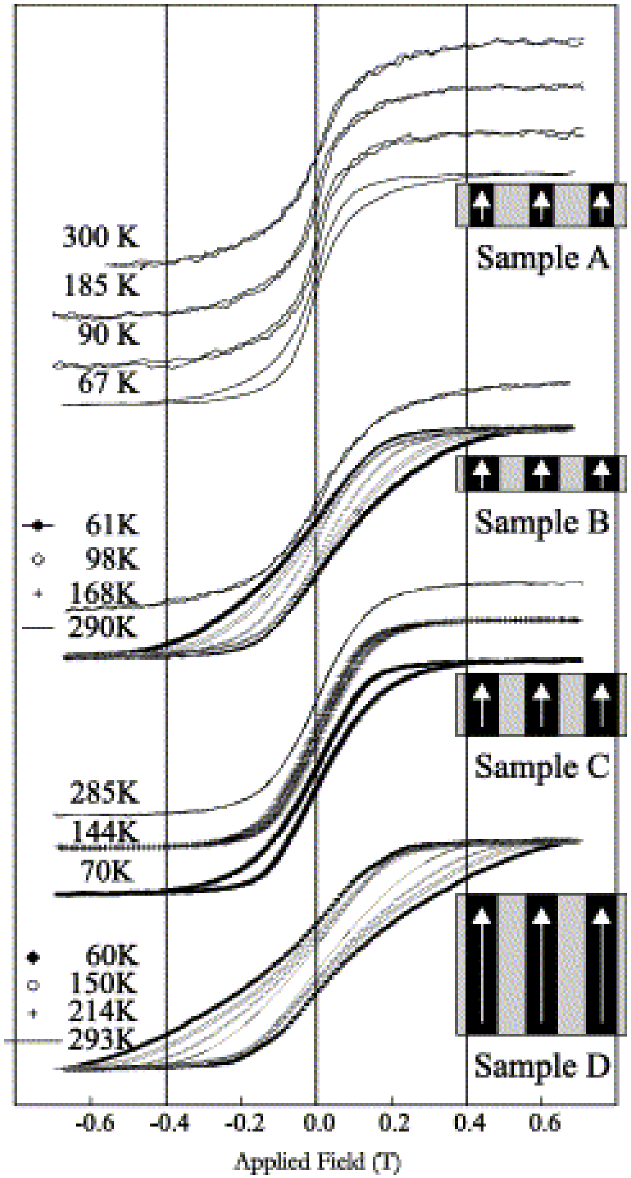

Limitations

Domain deformation approaching a (100) step:

- Coherence lost at step edges
- Rotated domains coehist on the same terrace

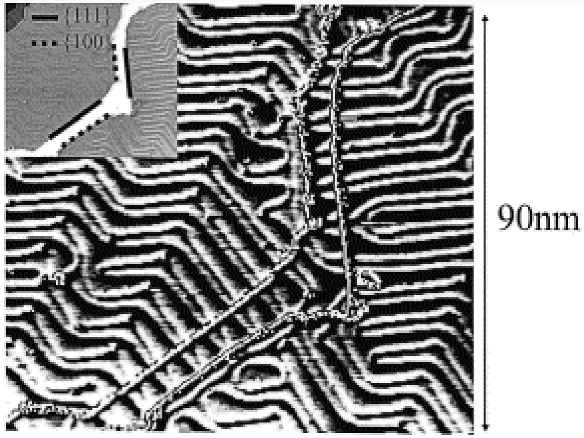

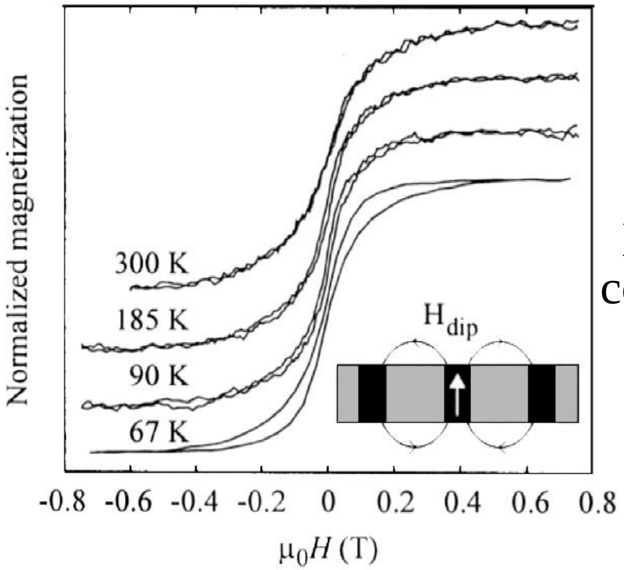

possible dipolar coupling: Hc does not change

Thermal stability vs MAE

VOLUME 71, NUMBER 21 PHYSICAL REVIEW LETTERS 22 NOVEMBER 1993

Thermally Activated Magnetization Reversal in Elongated Ferromagnetic Particles

Hans-Benjamin Braun

$$\mathcal{E} = \int_{-L/2}^{L/2} dx \left\{ \frac{A}{M_0^2} \left[(\partial_x M_x)^2 + (\partial_x M_y)^2 + (\partial_x M_z)^2 \right] + \frac{K_h}{M_0^2} M_z^2 - \frac{K_e}{M_0^2} M_x^2 - H_{\text{ext}} M_x \right\}$$

Exchange

Magnetic anisotropy (including the dipolar)

Uniform reversal

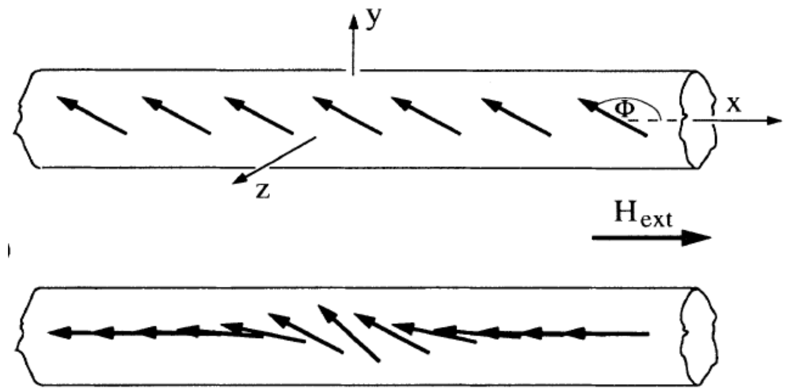

This solution is true in the limit of H_{ext} ->0

Reversal by domain wall creation and displacement

H.-B. Braun Phys. Rev B **50**, 16502 (1994);
H.-B. Braun Phys. Rev B **50**, 16485 (1994);
H.-B. Braun Phys. Rev Lett. **71**, 3557 (1993);
H.-B. Braun J. Appl. Phys. **85**, 6172 (1999);

Thermal stability vs MAE

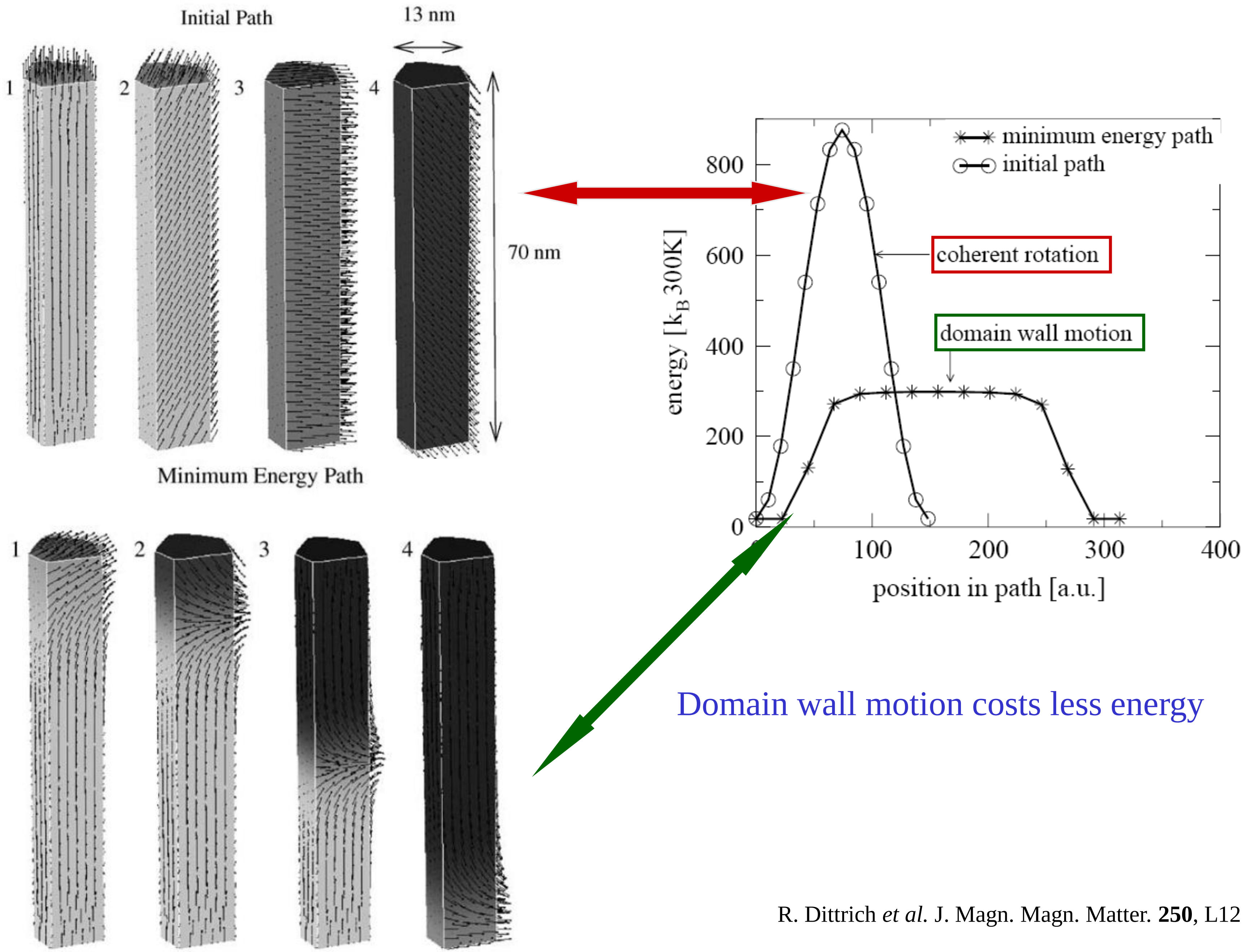

Domain wall motion costs less energy

R. Dittrich *et al.* J. Magn. Magn. Matter. **250**, L12 (2002)

Nanoparticle magnetization state: reversal state

Elongated islands switch faster than compact islands: different reversal mechanism

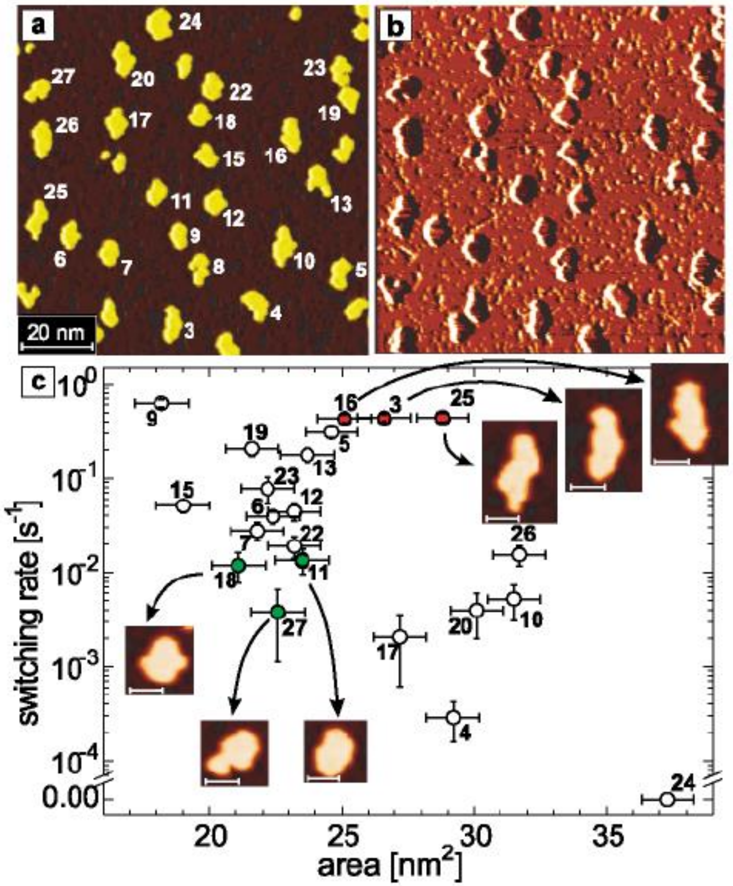

Spin Polarized-STM image of monolayer high Fe islands on Mo(110)

L_{crit} = 9 nm for Fe/Mo(110)

$L < L_{crit}$ -> Coherent rotation

$L > L_{crit}$ -> domain wall motion

$L_{crit} = 4\ \mathrm{sqrt}(J/K)$ if $K >> \mu_0 M^2$

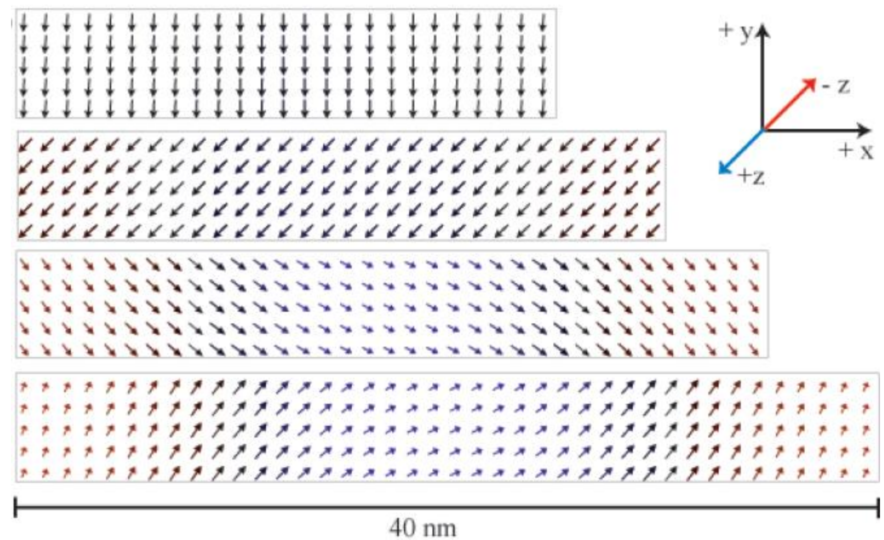

Micromagnetic simulation of Co islands on Pt(111)

M. Bode et al. Phys.Rev. Lett. **92**, 067201 (2004)

Vortex domain

Vortex domain are potential candidate for magnetic storage devices

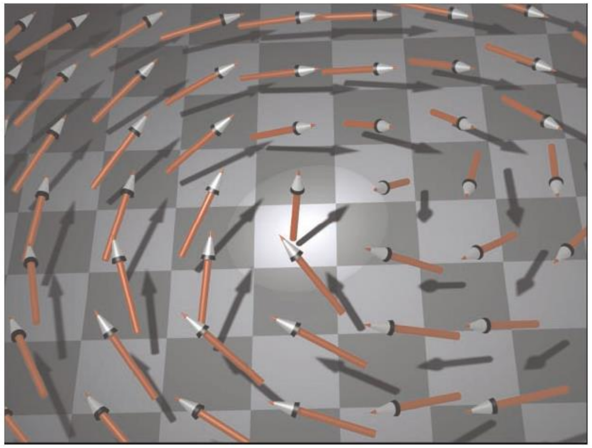

Vortex structure

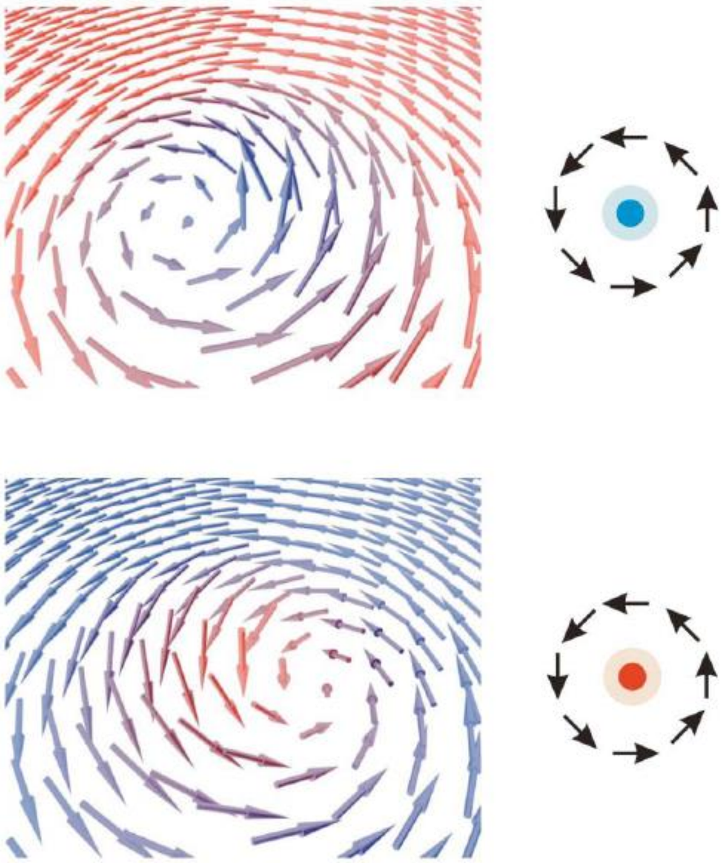

SP-STM image of a vortex structure

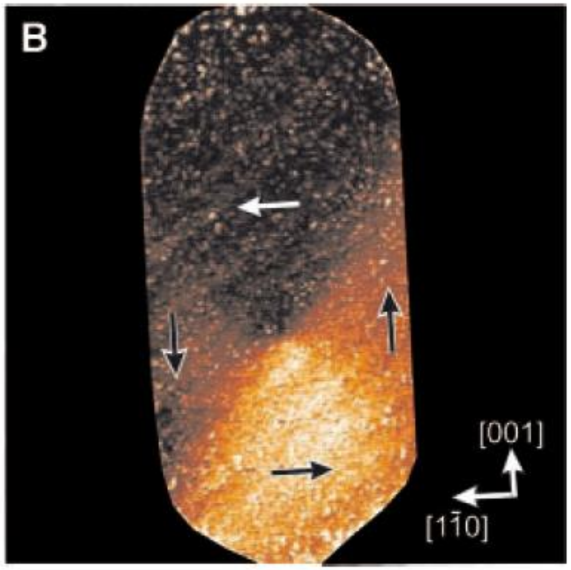

the out-of-plane polarization of the magnetic vortex core can be regarded as '0' or '1' of a bit element

B. Van Waeyenberge *et al*. Nature **444**, 461 (2006)
A. Wachowiak *et al*.. Science **298**, 577 (2002)

Real bit

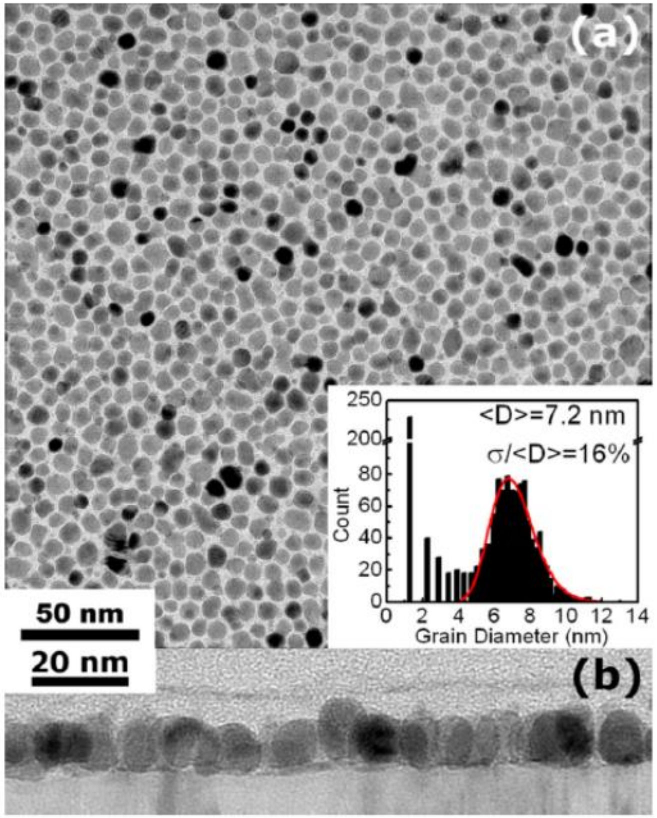

FIG. 2. (Color online) (a) Plan-view TEM image showing granular FePtAg-C media. The inset shows a histogram of the grain size distribution. The solid line in the inset shows a lognormal fit to the grain size distribution, which results in an average grain diameter $\langle D \rangle = 7.2$ nm and a grain size distribution $\sigma_D / \langle D \rangle = 16\%$. A cross-sectional TEM image is shown in (b). Note that the grains have a spherical shape.

O. Mosendz, *et al.* J. Appl. Phys. **111**, 07B729 (2012); D. E. Laughlin, *et al.* J. Appl. Phys. **105**, 07B739 (2009); R. Araki, et al. IEEE Trans. Magn. 44, 3496 (2008).

The inter-grain exchange interaction is stopped by the oxide layer

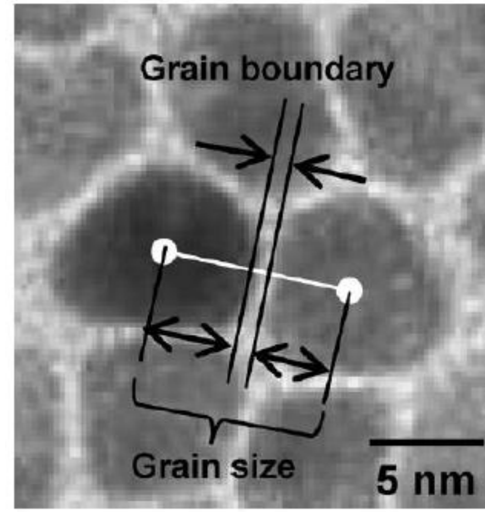

Tooth growth

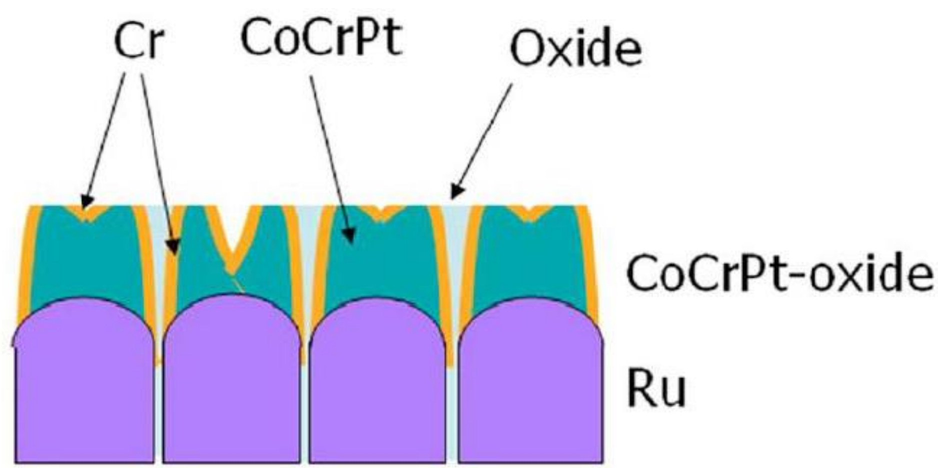

Real bit

Constraints on the magnetic grain:

1) Size below 8 nm
2) Uniform size distribution
3) Well defined boundary
4) Magnetically decoupled

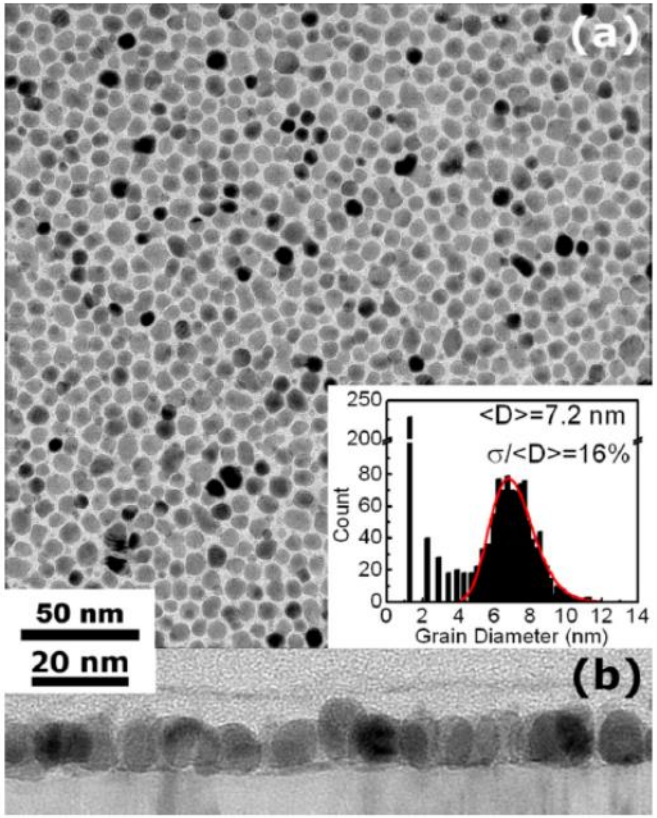

FIG. 2. (Color online) (a) Plan-view TEM image showing granular FePtAg-C media. The inset shows a histogram of the grain size distribution. The solid line in the inset shows a lognormal fit to the grain size distribution, which results in an average grain diameter $\langle D \rangle = 7.2$ nm and a grain size distribution $\sigma_D / \langle D \rangle = 16\%$. A cross-sectional TEM image is shown in (b). Note that the grains have a spherical shape.

The grain size distribution results in a rather wide switching field distribution

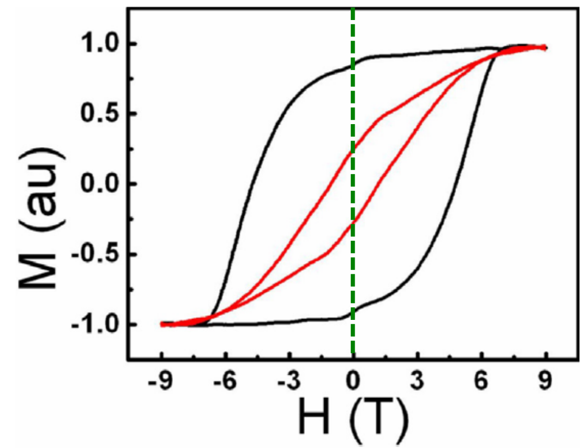

FIG. 3. (Color online) Easy and hard axis VSM magnetization loops measured at room temperature are shown with black and grey (red online) lines, respectively. A high coercive field $H_c = 4.85$ T was obtained for this sample with remanent magnetization above 90% of the saturation value. Note that the hard axis is not saturated at 9 T applied field and its amplitude was normalized to that of the easy axis loop for the highest applied field.

O. Mosendz, *et al.* J. Appl. Phys. **111**, 07B729 (2012); D. E. Laughlin, *et al.* J. Appl. Phys. **105**, 07B739 (2009); R. Araki, et al. IEEE Trans. Magn. 44, 3496 (2008).

Magnetic recording media

Conventional Media vs. Patterned Media

HITACHI Inspire the Next

Writing-reading head

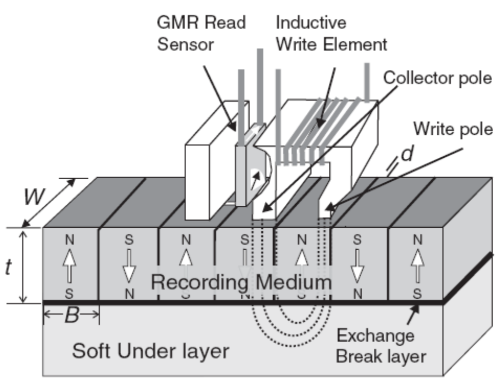

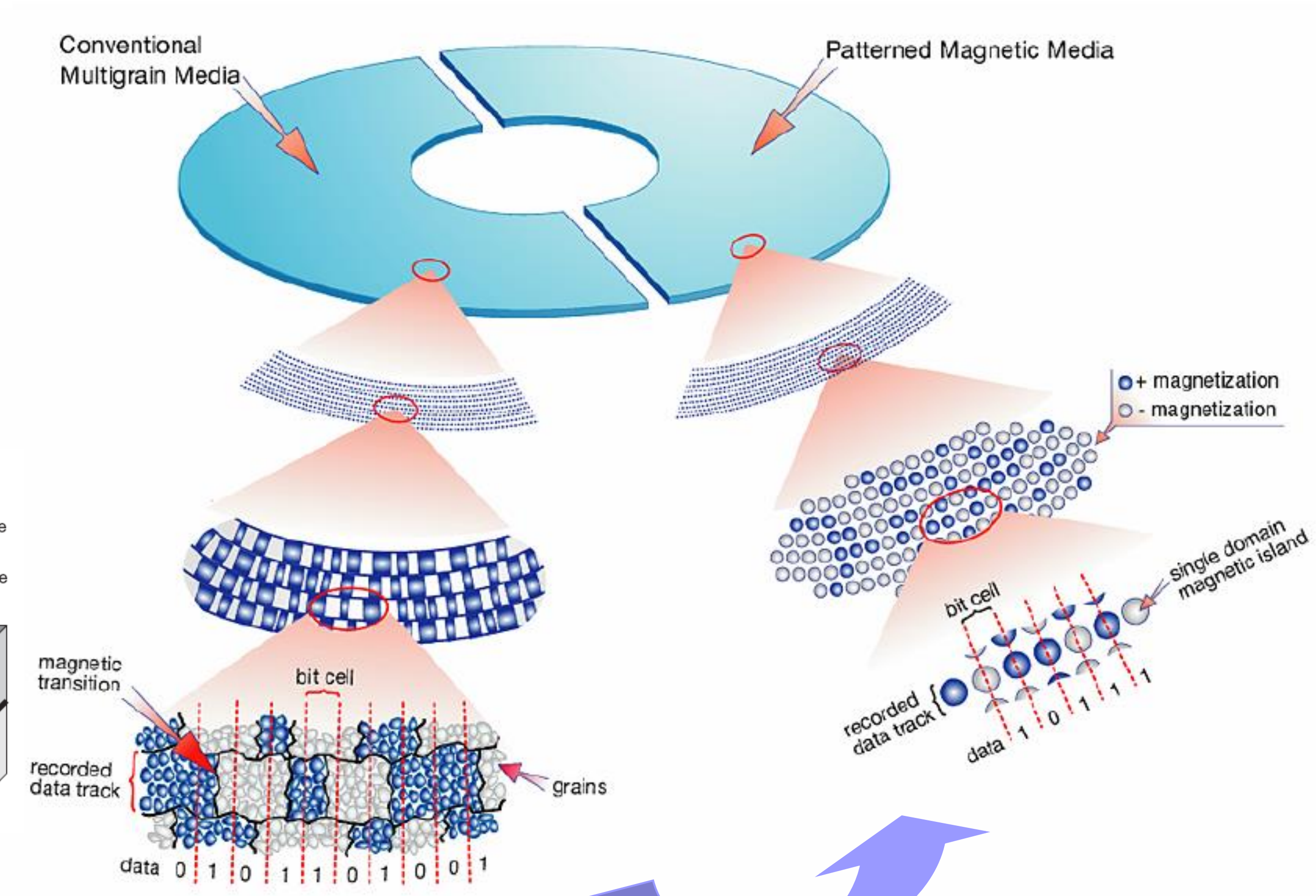

Each bit is made of a few hundreds of grains. The bit size and shape is defined during writing by the head

The future: single particle per bit